Ecosystem physio-phenology revealed using circular statistics

Changes in the manuscript

12-06-2020

Dear Editor,

Please find below our responses to the reviewers, a description of the major changes, and a detailed version of the manuscript with all the changes at the end of the document.

In the following, we repeat the **comments by the reviewers in bold** and our response (RS) to each one in normal font:

Responses to Reviewer 1:

Reviewer 1: In the manuscript entitled "Ecosystem physio-phenology revealed using circular statistics" submitted to Biogeosciences by Pabon-Moreno et al, the authors have performed an analysis of the timing of GPPmax across 52 flux sites using a circular regression method. The authors have also compared circular regression and linear regressing using simulated data and concluded the circular regression may be more suitable for these kinds of analysis.

Although the work is not of its first kind on the topic of circular stats for phenological modeling -as the authors have also pointed this out-, but the manuscript is still interesting. I believe the presentation of the work, however, can be much improved. There are also important questions and ambiguity about some of the technical parts of the manuscript that are not currently clear. In the manuscript, there are assumptions without proper justifications or performing sensitivity analysis for those assumptions. The presentations of the figures could also be improved. Overall, there is a lot of room for improvement.

We thank the reviewer for the comments. We agree that circular statistics have been used earlier for phenological analysis. However, in the specific context addressed in our paper (using ecosystem scale metrics inferred from eddy covariance towers) this is new, and we can provide some novel insights. We also would like to kindly point out that the comparison of circular vs. linear regressions is only one part of the entire work. The main research question is dedicated to understanding how climate conditions affect DOY_{GPPmax} - and the tool to address questions of this kind (circular regression) needs to be introduced properly. Regarding the technical aspects we solved all the doubts in the following questions. We kindly point out that the sensitivity analysis for the decay function was performed and is shown in Supplement 1. We clarify this in the manuscript. We also performed a new sensitivity analysis for the comparison between the circular and linear regression using a range of regression coefficients as suggested by the reviewer. The detailed changes are presented at the end of the manuscript.

- L18-19: the last sentence of the abstract is suggested to be rephrased, it kind of awkward.

We apologize for the awkward wording in the submitted draft which was: "In particular global analyses can benefit from this approach, i.e. when phase shifts play a role or double peaked growing seasons have to be considered." The sentence has now been rewritten as follows: "The analysis of phenological events at global scale can benefit from the use of circular statistics. Such an approach yields substantially more robust results for analyzing phenological dynamics in regions characterized by two growing seasons per year, or when the phenological event under scrutiny occurs between two years (i.e. DOY_{GPPmax} in the Southern Hemisphere)".

- L22: remove "e.g."

We remove the "e.g" and now the paragraph reads:

"Phenology is the study of the timing of biological events that can be observed either at the organismic level or at the ecosystem scale (Lieth, 1974). For the latter, phenology is the study of some integral behavior across phenological states of the integrated canopy reflectance captured by remote sensing (Richardson et al., 2009; Zhang et al., 2003), or vegetation-driven ecosystem-atmosphere CO2-exchange fluxes (Richardson et al., 2010)."

- L 45-48: "Bauerle et al. (2012) studied how photoperiod and temperature influence plants photosynthetic capacity, reporting that the photoperiod explains the variability of photosynthetic capacity better than temperature." Should mention study area, this is not a general fact, as it is a debated topic.

We thank the reviewer for the comment. We added the number of species and the area of this study.

Now the manuscript between line 45 and line 47 reads:

"Bauerle et al. (2012) studied how photoperiod and temperature influence plants photosynthetic capacity for 23 tree species in temperate deciduous hardwoods, reporting that the photoperiod explains the variability of photosynthetic capacity better than temperature."

-L74-78: What about the issue regarding southern vs northern hemisphere? earlier in the Introduction you discussed about it.

We thank the reviewer for pointing this out.It is correct that this aspect needs to be addressed here. However, we tone it a bit down given that the overarching research question is on understanding how climate variability affects DOY_{GPPmax}. We have rewritten the final part of the introduction as follows:

"In this paper, we aim to identify the factors controlling the timing of the maximal seasonal GPP (DOY_{GPPmax}). The questions we want to answer are: First, can circular statistics describe and predict DOY_{GPPmax} per vegetation type? This aspect requires testing the methodological advantages and caveats of circular statistics across hemispheres in comparison with linear methods. Second, can DOYGPPmax be explained using cumulative climate conditions? This question needs to consider different possibilities for generating temporally integrating features. And third, how is DOY_{GPPmax} affected by the climatic conditions during the growing season? The last question requires a global cross-site analysis. Based on the findings of these three questions we then discuss the potential of circular regressions beyond this specific application case in related phenological problems and outline future applications.

- L93: define i and tau, right after the equation.

We re-wrote the description of the equation including the definition of i and tau. Now it reads:

" We aggregate the original times-series of the Tair, SWin, Precip, and VPD for each DOY_{GPPmax} using a half-life decay function (eq. 1),

$$\langle \mathbf{x}_t \rangle = \frac{\sum_{i=0}^{\tau} x_{t-i} w_i}{\sum_{i=0}^{\tau-1} w_i} \quad (1)$$

for estimating an exponentially weighted mean of the observation vector, $\mathbf{x}_t = (x_t, x_{t-1}, \ldots, x_{t-\tau})^T$, at time step t. The symbol $\langle \cdots \rangle$ denotes the weighted average; i indicates the number of days before t going back up to $\tau = 365$ days.

- L96: Is w0=1? If so, you need to tell the readers.
Yes, we added w0 = 1 at line 100.

- L98: Not clear why you chose a decaying weight relationship, there should be a sensitivity analysis on how the results are affected by different weights. Your assumption is simply not justified.

We kindly point the reviewer to the supplement 1 where we documented a sensitivity analysis to identify the optimum decay weight per site as proposed here. To clarify this part, we re-wrote the paragraph that now reads:

"We perform a sensitivity analysis evaluating the effect of the half-time parameter and identify the optimum as the value when the variance explained by the circular regression model is maximum. The results are presented in Supplement 1"

- L109: Based on equation (2), y is the phase (angle) not DOY as it is introduced in the next line. You need a coefficient to transform.

To clarify this point, we added to the paragraph: "where *y* is the target variable (i.e. DOY_{GPPmax}) in radians", and we added at the beginning of the section:

“Since circular response variable must be in radians or degrees. We transform the days of the year to radians using equation 3. For leap years we remove the last day.”

$$rad = DOY \ \frac{360}{365} \ \frac{\pi}{180}$$

- L127: replace "artificial" with "simulated"

Yes, indeed.

- L128: Again, your choices of β1 = 0.3 and β2 = 0.1 are arbitrary, you need to do a sensitivity analysis and test the results for ranges of β1 and β2.

We thank the reviewer for this comment. To address this criticism we performed a completely new sensitivity analysis for a range of beta parameters values. We re-wrote the methods and result sections and introduced a new figure 3 in the submitted manuscript. At the end of the document we present the detailed changes of each section. In summary our results suggest that circular regressions can recover predefined coefficients in a set of simulations that represent realistic data with higher accuracy and precision than linear regressions. As was demonstrated with the previous analysis but this time, the evaluation of different beta regression coefficients will clarify that it’s not a local statistical artifact but even more a general tendency. One more time, thanks to the reviewer for suggesting the analysis.

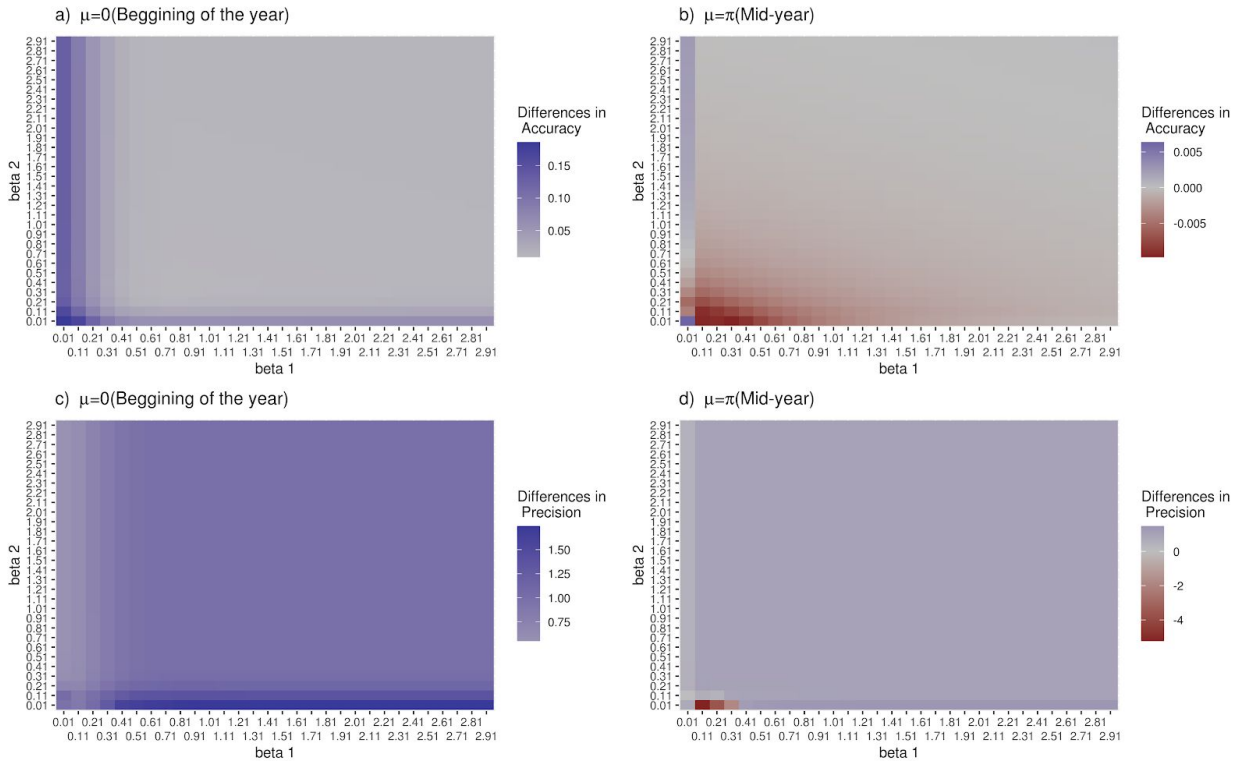

Figure 3. Accuracy and precision of linear and circular regression models by recovering the original regression coefficients of a circular regression. Left side: μ= 0(Maximum at the beginning of the year). Right side μ=pi(Maximum at Mid-year). a. and b. correspond to the differences in accuracy between the models. c. and d. correspond to the differences in the precision between the models. The blue color means better performance of the circular model compared with the linear model, and red color means higher performance of the linear model.

Figure 3 shows that for μ= 0 (DOY_{GPPmax} at the beginning of the year) circular regression has a higher accuracy and precision than the linear regression for the entire space of regression coefficient values, with a maximum difference in the order of 0.1 for the accuracy, and the order of 1 for the precision. For μ=π (DOY_{GPPmax} mid-year) linear model has a higher accuracy in most of the evaluated space with a maximum difference in the order of 0.001 compared with the circular regression. While, circular regression has a higher precision for most of the regression coefficients in the order of 0.001. These results show that circular regression has a higher precision to recover the original regression coefficients than linear regression no matter the moment of the year. On the other hand, circular regression has a higher accuracy than linear model at the beginning of the year. While at mid-year when linear is better the differences are in the order of 0.001.

- Figure 2: not a great figure. very difficult to follow, what is 6.697? I would redraw with a better idea.

We apologize for the lack of readability. Please note that 6.697 is the equal to -0.413 radians, we clarify this adding to the legend: "(The equivalent of -0.413 radians is 6.697. It is shown below the equation)". For us, the figure is important to show the effect of the increase in the variable when the regression coefficient is positive and negative. For this reason, we decided to include the equations with the plot and use the color to denote the increase.

- Figure 4: in (a) the circles are smashed to together so the trends are not very clear.

The transparency of the point can make the figure does not clear. With the use of density function for the distribution the outliers cannot be appreciated. Therefore, we would like to keep this figure. We also fixed the arrows in the figure because the counter parameter was setting wrongly before and the arrows were not showing the mean angular direction of the original data.

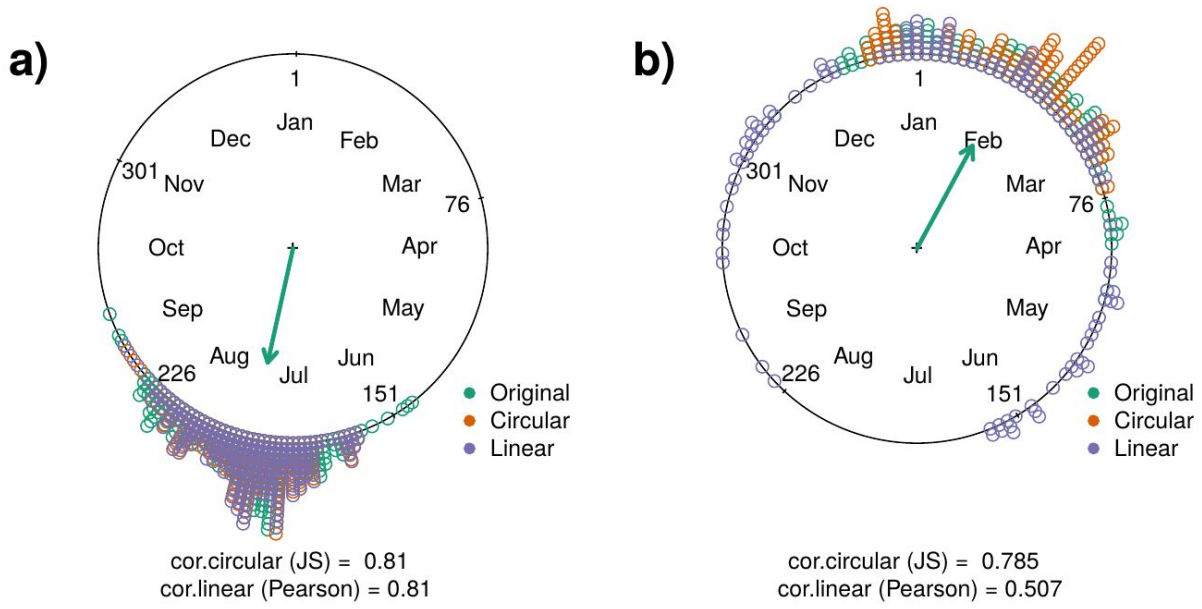

Figure 4. Correlation coefficient between the observed and predicted DOY_{GPPmax} using climatic variables. Two sites are presented: a. US-Ha1, and b. AU-How. The observed DOY_{GPPmax} (Green) is compared with the data retrieved using Circular (Orange) and Linear (Purple) regressions. Two correlation coefficients are used: Jammalamadaka-Sarna (JS) and Pearson product-moment (Pearson). In the circular plot the months and the day of the year (DOY) are also plotted every 75 days. The green arrow indicates the mean angular direction of the original data distribution.

- L202: What is "the power of the prediction"? vague term.

We rewrote this term as “predictive power”. That is a well-established term to describe the property of a mathematical model to predict a specific event.

- Figure 7: Another figure to be improved. The smoothed curves do not add anything. It is not even clear how they are obtained or if there is any quantitative metric to see the fit. See EBF for instance. I would get rid of them. Also, the plots must have square aspect ratio.

We thank the reviewer for the comment. We removed the tendency lines to avoid confusion, replotted using the square aspect ratio and moved the JS correlation coefficient to the title of each plot.

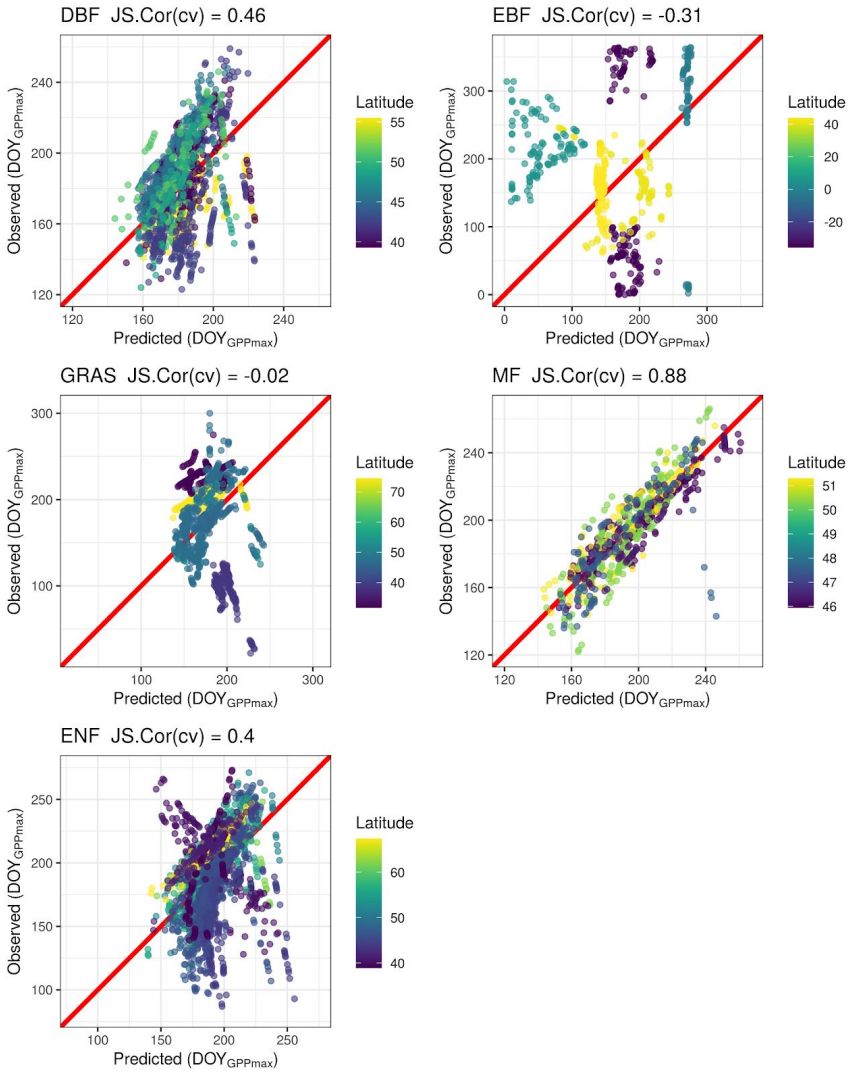

Figure 7. Cross validation of the circular regression model to predict DOY_{GPPmax} for different vegetation types using air temperature, short-wave incoming radiation, precipitation and vapor pressure deficit (see methods). Deciduous Broadleaf Forest (DBF). Evergreen BroadleafForest (EBF). Grassland (GRA). Mixed Forest (MF), and Evergreen Needleleaf Forest (ENF). For each vegetation type the Jammalamadaka-Sarna (JS) correlation coefficient is shown in the title of each plot. The red line represents the perfect fit.

- L214: The sentence referred to a paper from 2013, and "concluded that phenology models need to be improved". In fact, there has been much improvements on phenology models since then.

We thank the reviewer for the comment. We re-wrote this paragraph (between lines 247 and 253) and now it reads:

“Different phenological models have been developed ranging from empirical approaches (Richardson et al., 2013) to process models (Asse et al., 2020) over the last decades. As we demonstrate here, circular statistics opens new opportunities to increase the robustness of phenological models allowing to analyze ecosystems across hemispheres within the same consistent frame-work. In fact, the results on phenological sensitivity of DOY_{GPPmax} indicate the complexity of ecosystem responses to climate variability. Our approach is a motivation towards integrating circular regressions into more complex statistical techniques like regression trees, Gaussian process, or artificial neural networks, targeting a circular response variable.”

- L217-218: "Indeed we considered our approach as a first step to implement more complex statistical techniques like decision trees, Gaussian process, or artificial neural networks, targeting a circular response variable." But the authors have not showed us how. From the manuscript, the connection between the circular regression and other methods mentioned here is not clear.

We re-wrote this phrase and now it reads:

“Our approach is a motivation towards integrating circular regressions into more complex statistical techniques like regression trees, Gaussian process, or artificial neural networks, targeting a circular response variable”

We include this phrase as an outlook, to clarify that even if circular methods contribute to understanding phenological events, there is a lot of space where models can be improved. And as a motivation to the reader to keep contributing in this field.

Major Changes

We re-wrote the methods and results of the section 2.3 Circular vs. Linear Regression; the new version is presented below and in the new version of the manuscript.

Circular vs. Linear Regression

To assess the performance of linear versus circular regressions we perform an experiment with simulated data where we evaluate the accuracy and precision of both approaches to recover original regression coefficients in a circular setting (eq. 4). We add noise generated with a random von Mises distribution with parameters: $n = 100$ and $\kappa = 30$ to the model to ensure that the result follows a normal distribution. We predefined a range of values for two regression coefficients ($\beta_1 = \langle 0.01, \ldots, 3 \rangle$, $\beta_2 = \langle 0.01, \ldots, 3 \rangle$). We simulate the variables x_1 and x_2 as normal distributions with $n = 100$, a mean of 10, and 15 respectively, and standard deviations of 1 and 2. We evaluate all possible combinations for the regression coefficients 100 times simulating different x_1 and x_2. In each iteration we generate y using the set-up previously described, and we recover the original regression coefficients using y as response variable and x_1 and x_2 as predictors. Finally, We analyze two scenarios: 1) when the target timing occurs at the beginning of the year ($\mu = 0$), and 2) when the target timing happens at mid-year ($\mu = \pi$). The parameters for the entire set-up generate realistic data where the standard deviation of y is not higher than 0.3 radians. A standard deviation of 0.5 radians would be equivalent to having phenological observations across half a year which would not be realistic.

To quantify the accuracy of each model per coefficient we estimate the mean absolute error per model and coefficient (eq. 5). To compare the accuracy between models by coefficient we rest the mean absolute errors between models (eq. 6). To generate a single measure that allows to compare both coefficients and models we estimate the mean difference accuracy (eq. 7). The results can be understood as follows: if the difference is higher than 0, the circular model has a higher mean accuracy compared to the linear model and vice versa. To quantify which model has higher precision we estimate the difference between the standard deviation of the mean absolute errors per model for each coefficient (eq. 8). Finally, we estimate the mean differences of precision between the regression coefficients (eq. 9) where again if the value is higher than 0 circular model has a higher mean accuracy than linear model and the inverse sense if the value is lower than 0.

We estimate regression coefficients for the bootstrap sample $i \in \{1, \ldots, m\}$, $m = 100$, for the regression coefficient β_j, $j \in \{1, 2\}$, and the model $M \in \{l, c\}$ (denoted as $\hat{\beta}_{j,i}^{M}$). The model accuracy can then be estimated as the mean absolute error of the estimated regression parameter $\hat{\beta}_j^M$, $j \in \{1, 2\}$ for the linear model, $M = l$, and the circular model, $M = c$:

$$a_{M,j} = \frac{1}{m}\sum_{i=1}^{m} |\hat{\beta}_{j,i}^{M} - \beta_j| \tag{5}$$

The difference in accuracy for the coefficient j between the circular and the linear model is shown in

$$\delta_{a,j} = a_{l,j} - a_{c,j} \tag{6}$$

Finally, the mean difference accuracy between the linear and the circular model is given by

$$\delta_a = \frac{\delta_{a,1} + \delta_{a,2}}{2} \tag{7}$$

The difference in precision for the coefficient j between the linear (l) and the circular model (c) is given by

$$\delta_{p,j} = \mathrm{s}_{l,j} - \mathrm{s}_{c,j} \tag{8}$$

The mean difference precision between the linear and the circular model is given by

$$\delta_p = \frac{\delta_{p,1} + \delta_{p,2}}{2} \tag{9}$$

Where $\mathrm{s}_{M,j}$ is the sample standard deviation of the vector $(\hat{\beta}_{j,i}^{M})_i$, $M \in \{l, c\}$.

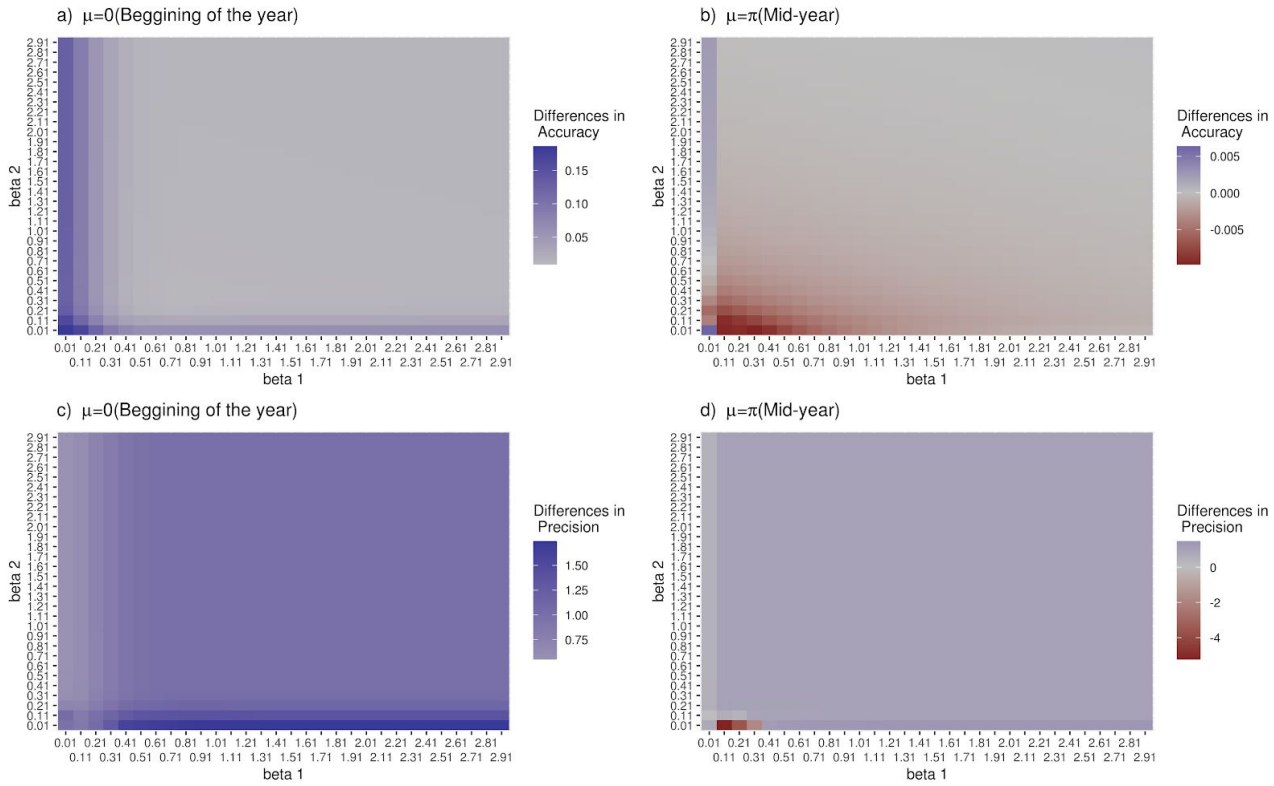

Figure 3. Accuracy and precision of linear and circular regression models by recovering the original regression coefficients of a circular regression. Left side: μ= 0(Maximum at the beginning of the year). Right side μ=pi(Maximum at Mid-year). a. and b. correspond to the differences in accuracy between the models. c. and d. correspond to the differences in the precision between the models. The blue color means better performance of the circular model compared with the linear model, and red color means higher performance of the linear model.

Figure 3 (a,c) shows that for μ= 0 (DOY_{GPPmax} at the beginning of the year) circular regression has a higher accuracy and precision than the linear regression for the entire space of regression coefficient values, with a maximum difference in the order of 0.1 for the accuracy, and the order of 1 for the precision. For μ=π (DOY_{GPPmax} mid-year) linear model has a higher accuracy in most of the evaluated space with a maximum difference in the order of 0.001 compared with the circular regression. While, circular regression has a higher precision for most of the regression coefficients in the order of 0.001. These results show that circular regression has a higher precision to recover the original regression coefficients than linear regression no matter the moment of the year. On the other hand, circular regression has a higher accuracy than linear model at the beginning of the year. While at mid-year when linear is better the differences are in the order of 0.001.

Ecosystem physio-phenology revealed using circular statistics

Daniel E. Pabon-Moreno[1], Talie Musavi[1], Mirco Migliavacca[1], Markus Reichstein[1,2], Christine Römermann[2,3], and Miguel D. Mahecha[1,2,4]

[1]Max Planck Institute for Biogeochemistry, 07745 Jena, Germany
[2]German Centre for Integrative Biodiversity Research (iDiv), Deutscher Platz 5e, 04103 Leipzig, Germany
[3]Friedrich Schiller University, Institute of Ecology and Evolution, Philosophenweg 16, D-07743 Jena, Germany
[4]Remote Sensing Center For Earth System Research, Leipzig University and Helmholtz-Centre for Environmental Research - UFZ, 04103 Leipzig, Germany

Correspondence: Daniel E. Pabon-Moreno (dpabon@bgc-jena.mpg.de)

Abstract. Quantifying how vegetation phenology responds to climate variability is a key prerequisite to predict how ecosystem dynamics will shift with climate change. So far, many studies have focused on responses of classical phenological events (e.g. budburst or flowering) to climatic variability for individual species. Comparatively little is known on the dynamics of physio-phenological events such as the timing of maximum gross primary production (DOY_{GPPmax}), i.e. quantities that are relevant for understanding terrestrial carbon cycle responses to climate variability and change. In this study, we aim to understand how DOY_{GPPmax} depends on climate drivers across 52 eddy-covariance (EC) sites in the FLUXNET network for different regions of the world. Most phenological studies rely on linear methods that cannot be generalized across both hemispheres and therefore do not allow for deriving general rules that can be applied for future predictions. One solution could be a new class of circular-linear (here called circular) regression approaches. Circular regression allows relating circular variables (in our case phenological events) to linear predictor variables as climate conditions. As a proof of concept, we compare the performance of linear and circular regression to recover original coefficients of a predefined circular model on artificial data. We then quantify the sensitivity of DOY_{GPPmax} across FLUXNET sites to air temperature, short-wave incoming radiation, precipitation and vapor pressure deficit. Finally, we evaluate the predictive power of the circular regression model for different vegetation types. Our results show that the joint effects of radiation, temperature and vapor pressure deficit is the most relevant controlling factor of DOY_{GPPmax} across sites. Woody savannas are an exception where the most important factor is precipitation. Although the sensitivity of the DOY_{GPPmax} to climate drivers is ~~very~~ site specific, it is possible to generalize the circular regression models across specific vegetation types. From a methodological point of view, our results reveal that circular regression is a robust alternative to conventional phenological analytic frameworks. ~~In particular global analyses~~ The analysis of phenological events at global scale can benefit from ~~this approach~~ the use of circular statistics. Such an approach yields substantially more robust results for analyzing phenological dynamics in regions characterized by two growing seasons per year, or when the phenological event under scrutiny occurs between two years (i.e. ~~when phase shifts play a role or double peaked growing seasons have to be considered~~DOY_{GPPmax} in the Southern Hemisphere).

1 Introduction

Phenology is the study of the timing of biological events that can be observed either at the organismic level or at the ecosystem scale (Lieth, 1974). For the latter, phenology is the study of some integral behavior across phenological states of ~~e.g.~~ the integrated canopy reflectance captured by remote sensing (Richardson et al., 2009; Zhang et al., 2003), or vegetation-driven ecosystem-atmosphere CO_2-exchange fluxes (Richardson et al., 2010). Ecosystem scale physio-phenological processes of this kind are relevant quantities in global biogeochemical cycles and integrates both, the seasonal dynamics of biophysical states (e.g. reflected in the canopy development), and the observed photosynthesis at the stand level (i.e. gross primary production). Here we are particularly interested in the timing when ecosystems reach their maximum CO_2-uptake ~~potential~~ within a growing season. ~~Note that the maximum CO_2-uptake potential does not necessarily coincide with the realized maximum GPP which is essentially driven by actual meteorological conditions (Musavi et al., 2016).~~ Ecosystem-physiophenology is influenced by climate conditions but simultaneously contributes to the regulation of different micro and macro meteorological ~~conditions~~patterns. Physio-phenological cycles determine the temporal dynamics of land-atmosphere water and energy exchange fluxes. Likewise, the terrestrial carbon cycle is affected by phenological controls on CO_2 uptake and release (Peñuelas et al., 2009).

The eddy covariance technique (EC) allows to continuously measuring the exchange of energy and matter between ecosystems and atmosphere (Aubinet et al., 2012). The FLUXNET network collects EC data for most ecosystems of the world along with other meteorological variables, i.e. radiation, temperature, precipitation, as well as with atmospheric humidity, and often soil moisture (Baldocchi et al., 2001; Baldocchi, 2020). Particularly relevant to pheneological studies is the seasonal trajectory of gross primary production (GPP) allowing to derive phenological transition dates such as start and end of the growing season (e.g., Luo et al., 2018), as well as the timing of the maximum gross primary production, hereafter as referred to as DOY_{GPPmax} (Zhou et al., 2016; Peichl et al., 2018; Wang and Wu, 2019).

In this study we focus on understanding how climate variability affects the time when ecosystems reach their maximum potential for CO_2 absorption. In order to reach this "optimum state" several preconditions must be met during the preceding part of the growing season. So far several studies have focused on studying the variability of maximum GPP during the growing season (GPPmax). For instance, Zhou et al. (2017) studied how the variability of annual GPP is influenced by GPPmax and the start and the end of the growing season. The authors found that GPPmax is a better explanatory parameter for the inter-annual variability of annual GPP than the start and end days of the growing season. Bauerle et al. (2012) studied how photoperiod and temperature influence plants photosynthetic capacity for 23 tree species in temperate deciduous hardwoods, reporting that the photoperiod explains the variability of photosynthetic capacity better than temperature. So far, to the best of our knowledge, only one study has focused on understanding the temporal variability of GPPmax: Wang and Wu (2019) used a combination of satellite remote sensing, and eddy-covariance data to explore how DOY_{GPPmax} is controlled by climatic conditions. The authors reported that higher temperatures advance DOY_{GPPmax}, while the influence of precipitation and radiation were biome-dependent. This study had a geographical focus on China; a global approach considering several ecosystems across the whole latitudinal gradient is still lacking.

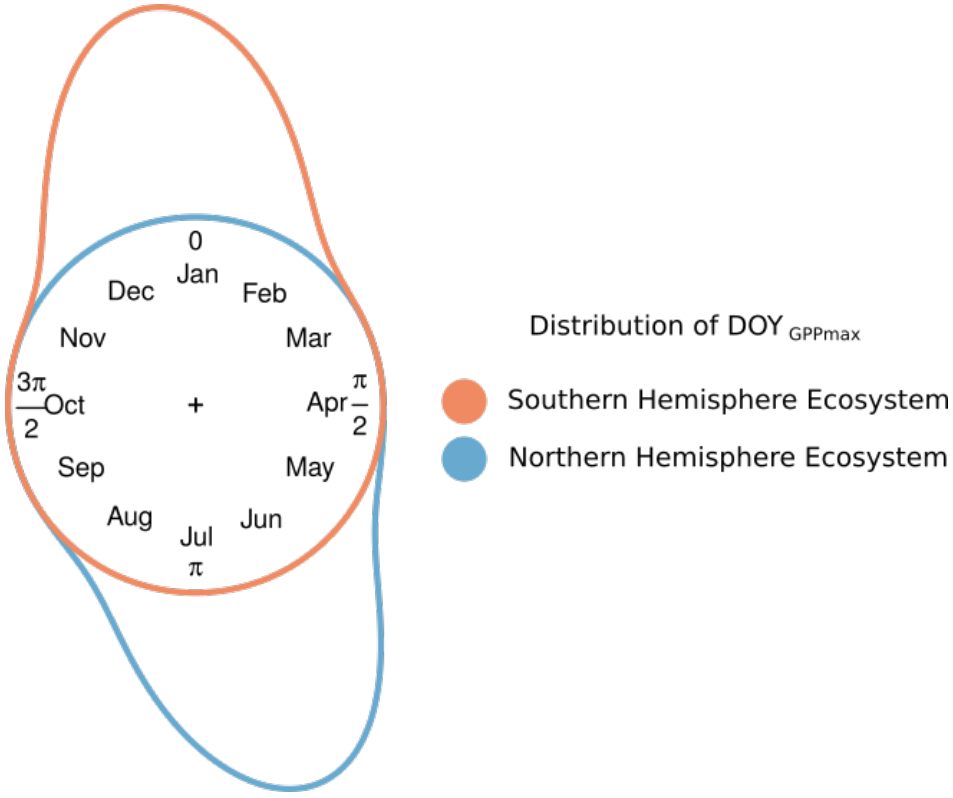

Figure 1. Conceptual distribution of GPPmax timing (DOY_{GPPmax}) for two hypothetical ecosystems one in the Northern (Blue), and one in the Southern Hemisphere (Red). The distance between the color line and the circle represent the frequency of the DOY_{GPPmax} observations. The distance between the end and the beginning of the distribution represent the DOY_{GPPmax} inter-annual variability.

The challenge of understanding phenology is generally to characterize a discrete event that repeats ~~with characteristic periodicity~~periodically. Classically, phenological analyses have been performed using linear regression models (Morente-López et al., 2018; Zhou et al., 2016). Most of these studies analyze ecosystems characterized by one growing season (e.g. temperate or boreal forests), and when the summer is centered around the middle of the calendar year. The existing methods are, however, not sufficiently generic to describe i) ecosystems in the Southern Hemisphere, and ii) ecosystems with multiple growing seasons per year as it is often observed in e.g. semi-arid regions.

Figure 1 illustrates the problem of Northern vs. Southern Hemispheric summers from a conceptual point of view. Assume that some discrete event recurs annually, but the timing varies according to some external drivers. We would then need to find a predictive model explaining the inter-annual variability of phenology i.e. the probability of this recurrent event in the course of the annual cycle. The Fig. 1 shows that linear regression models would be inappropriate to predict the day of the year (DOY) of some phenological event in the Southern Hemisphere, as the actual target values to predict may flip between $\gtrapprox \frac{3\pi}{2}$ and $\lessapprox \frac{\pi}{2}$.

In recent years, circular statistics have gained some attention as they offer a solution to problems of this kind (Morellato et al., 2010; Beyene et al., 2018). Unlike classical statistics, the predicted variables are expressed in terms of angular directions (degrees or radians) across a circumference (Fisher, 1995) allowing to perform statistical analysis where the data space is not Euclidean. In this framework, point events can be described as a von-Mises distribution (Von Mises, 1918), the equivalent to the normal distribution in the circular statistics. The von-Mises distribution is described by two parameters: The mean angular direction (μ) and the concentration parameter (κ). Circular-linear regressions (in the following simply named circular regression) allow to predict circular responses (e.g. the timing of phenological events) from other linear variables (Morellato et al., 2010). Given that any phenological event can be interpreted as an angular direction, and should be modeled alike, we assume that these circular regressions are well suited in this context. Despite this evident suitability, circular statistics have not yet been extensively applied in the study of phenology and will therefore be presented here as an alternative to conventional linear techniques.

In this paper, we aim to identify the factors controlling the timing of the maximal seasonal GPP (DOY_{GPPmax}). The questions ~~that~~ we want to answer are: First, can circular statistics describe and predict DOY_{GPPmax} per vegetation type? ~~Can~~ This aspect requires testing the methodological advantages and caveats of circular statistics across hemispheres in comparison with linear methods. Second, can DOY_{GPPmax} be explained using cumulative climate conditions? ~~How~~ This question needs to consider different possibilities for generating temporally integrating features. And third, how is DOY_{GPPmax} affected by the climatic conditions during the growing season? ~~Based on these findings we~~ The last question requires a global cross-site analysis. Based on the findings of these three questions we then discuss the potential of circular regressions beyond this specific application case in related phenological problems and outline future applications.

2 Methods

2.1 Data

We use 52 EC sites (with at least seven years of data) located through the latitudinal gradient of the globe from the FLUXNET-2015 database (Table A1, http://fluxnet.fluxdata.org/ Pastorello et al., 2017). Each FLUXNET site is identified with an abbreviation of the country and the name of the place e.g. the EC tower AU-How, means that it is located in Howard Springs, Australia. From the dataset we use the GPP data that was derived using the nighttime partitioning method and considering the variable $u^{\star}$-threshold to discriminate values of insufficient turbulence (Reichstein et al., 2005). In order to identify maximum daily GPP, we compute the quantile 0.9 for each day based on the half-hourly flux observations. As potential explanatory variables for DOY_{GPPmax} we use the daily air temperature (Tair), shortwave incoming radiation (SWin), precipitation (Precip), and vapor pressure deficit (VPD).

Given that the past climate conditions affect the CO_2 exchange between the atmosphere (ecological memory, Liu et al., 2019; Ryan et al., 2015), we assume that an aggregated form of these climatic variables needs to be considered in the prediction of

the phenological responses. We aggregate the original times-series of the Tair, SWin, Precip, and VPD for each DOY_{GPPmax} using a half-life decay function (eq. 1):

$$\left\langle x_{\mathbf{t}} \right\rangle = \frac{\sum_{i=0}^{\tau} x_{t-i} w_i}{\sum_{i=0}^{\tau-1} w_i} \quad , \tag{1}$$

where $\langle x \rangle$ denotes the for estimating an exponentially weighted mean of the vector of observations $x = (x_t, x_{t-1}, \ldots, x_{t-\tau})^T$ with exponentially decaying weights

$$w_i = w_0 e^{-i \frac{ln(2)}{t_{1/2}}}$$

This approach assigns a lower weight the further we go back in time to a maximum of τ days ($\tau = 365$) before the observation vector, $\mathbf{x}_t = (x_t, x_{t-1}, \ldots, x_{t-\tau})^T$, at time step t that is set to the DOY_{GPPmax}. We can then vary the half-time parameter ($t_{1/2}$) from 2 to 365. The symbol $\langle \ldots \rangle$ denotes the weighted average; i indicates the number of days before t going back up to $\tau = 365$ days. The weight decay is represented by

$$w_i = w_0 \exp\left(-i \frac{ln(2)}{t_{1/2}}\right) \quad . \tag{2}$$

The decay function give the instantaneous value a weight of 1 and, ($w_0 = 1$) and all preceding values receive an exponentially reduced weight as determined by the half-time-parameter $t_{1/2}$. We Finally, we make these variables comparable via centering standardization to unit variance. We perform a sensitivity analysis evaluating the effect of the half-time parameter and identify the optimal $t_{1/2}$ to increase optimum as the value when the variance explained by the circular-regression model using the Jammalamadaka-Sarma (JS) correlation coefficient (Jammalamadaka and Sarma, 1988) (Supplement 1). circular regression model is maximum. The results are presented in Supplement 1.

Due to the high co-linearity between the exponential weighted variables of Tair, SWin and VPD we perform a principal component analysis (PCA) on the matrix of variables and FLUXNET sites and retain the leading principal component of these variables, and precipitation as input for the circular statistics model (Hastie et al., 2009). The results of the PCA analysis are presented in the Supplement 2.

2.2 Circular statistics

Since units of the circular response variable must be in radians or degrees. We transform the days of the year to radians using equation 3. For leap years we remove the last day.

$$rad = DOY \frac{360}{365} \frac{\pi}{180} \tag{3}$$

where DOY : Day of the year.

A basic circular regression model was proposed by Fisher and Lee (1992) as follows:

$$y = \mu + 2\,\mathrm{atan}(\beta_i x_i) \tag{4}$$

where y is the target variable (i.e. $\mathrm{DOY}_{\mathrm{GPPmax}}$) ~~,~~ in radians. μ is the mean angular direction of the target variable, x_i are the values for the variable i, and β_i is the regression coefficient. The parameters μ and β are fitted via the maximum likelihood method using reweighted least squares algorithm as proposed by Green (1984).

Relevant interpretations of fitted circular regression models are 1) the sign of the β-coefficients, 2) the statistical significance of the coefficients, and 3) the accuracy of the prediction. Regarding the first point: A negative sign of the coefficient would mean that an increasing value of the predictor would lead to an earlier $\mathrm{DOY}_{\mathrm{GPPmax}}$ compared to the mean angular direction. The inverse would happen when the coefficient is positive. Figure 2 conceptually illustrates how the coefficients affect the predictions. Regarding the second aspect we can state that, if a coefficient is not significant, then its contribution would not be relevant to explain the phenological observation. In our case we define that the coefficient is significant if the median of the distribution of p-values is less than 0.05. Finally, we can estimate the accuracy of the prediction using the Jammalamadaka-Sarma (JS) correlation coefficient (Jammalamadaka and Sarma, 1988). As in any other regression framework, this approach helps us to quantify the effect of each climate variable on the inter-annual variability of $\mathrm{DOY}_{\mathrm{GPPmax}}$.

To estimate the relative sensitivity of $\mathrm{DOY}_{\mathrm{GPPmax}}$ to the leading principal component representing Tair, SWin, and VPD, as well to Precip we use the implementation of equation 4 in the R package "circular" (Agostinelli and Lund, 2017). To ~~assess~~ increase the robustness of the method we implemented a block bootstrapping per growing season generating a model parameter average based on 1000 iterations. In each analysis, we estimate the accuracy of the model using the JS correlation coefficient.

2.3 Circular vs. Linear Regression

To assess the performance of linear versus circular regressions we ~~performed a small experiment with artificial data : We use equation 4 where we predefine two coefficient regressions ($\beta_1 = 0.3, \beta_2 = 0.1$~~perform an experiment with simulated data where we evaluate the accuracy and precision of both approaches to recover original regression coefficients in a circular setting (eq. 4). We add noise generated with a random von Mises distribution with parameters: $n = 100$ and $\kappa = 30$ to the model to ensure that the result follows a normal distribution. We predefined a range of values for two regression coefficients ($\beta_1 = \langle 0.01, \ldots, 3 \rangle$, $\beta_2 = \langle 0.01, \ldots, 3 \rangle$). We ~~generate~~ simulate the variables x_1 and x_2 as normal distributions with $n = 100$, a mean of 10, and 15 respectively, and standard deviations of 1 and 2. We evaluate all possible combinations for the regression coefficients 100 times simulating different x_1 and x_2. In each iteration we generate y using the set-up previously described, and we recover the original regression coefficients using y as response variable and x_1 and x_2 as predictors. Finally, We analyze two scenarios: 1) when the target timing occurs at the beginning of the year ($\mu = 0$), and 2) when the target timing happens at mid-year ($\mu = \pi$). ~~We simulate the variables x_1 and x_2 as normal distributions with a mean of~~ The parameters for the entire set-up generate realistic data where the standard deviation of y is not higher than 0.3 radians. A standard deviation of 0.5 radians would be equivalent to having phenological observations across half a year which would not be realistic.

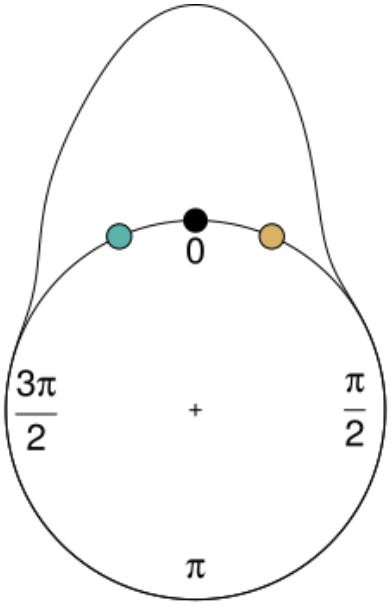

μ		β_1	X_1	β_2	X_2
0	= 0 + 2 atan(-0.3 ×	0.6	+ 0.3 ×	0.6)	
-0.413	= 0 + 2 atan(-0.3 ×	1.3	+ 0.3 ×	0.6)	
6.697					
0.413	= 0 + 2 atan(-0.3 ×	0.6	+ 0.3 ×	1.3)	

Figure 2. Interpretation of the coefficients in the circular regression. Consider a reference point (Black) generated with a circular-linear model with mean angular direction ($\mu = 0$), two coefficients (β_1,β_2) and two variables (x_1, x_2), where one of the coefficients is negative (β_1) and the other one is positive (β_2). When the coefficient is negative and the value of the parameter increases (blue) the result is an earlier observation compared with the reference point (The equivalent of ~~the negative radian~~ -0.413 radians is 6.697 radians. It is shown below the equation). On the other hand, when the coefficient is positive and the variable increase (yellow) the observation is later.

To quantify the accuracy of each model per coefficient we estimate the mean absolute error per model and coefficient (eq. 5). To compare the accuracy between models by coefficient we rest the mean absolute errors between models (eq. 6). To generate a single measure that allows to compare both coefficients and models we estimate the mean difference accuracy (eq. 7). The results can be understood as follows: if the difference is higher than 0~~, and 4 respectively, and set them to unit variance. For each scenario the number of data is given by the equation ?? where n (rounded)is~~ , the circular model has a higher mean accuracy compared to the ~~amount of data for x_1 and x_2 and d take arbitrary values from 5 to 1000.~~

$n = e^{\log(d)}$

~~We use the simulated data from equation 4, and~~ linear model and vice versa. To quantify which model has higher precision we estimate the difference between the standard deviation of the ~~original values of x_1 and x_2 to recover the original values of~~

mean absolute errors per model for each coefficient (eq. 8). Finally, we estimate the mean differences of precision between the regression coefficients ~~β_1 and β_2 using the circular and linear regression. To increase the robustness of the analysis we simulate x_1 and x_2 1000 times for each amount of data. We estimate the difference between the recovered and the original coefficient divided by~~ (eq. 9) where again if the value is higher than 0 circular model has a higher mean accuracy than linear model and the inverse sense if the value is lower than 0.

We estimate regression coefficients for the bootstrap sample $i \in \{1,\dots,m\}$, $m = 100$, for the regression coefficient β_j, $j \in \{1,2\}$, and the model $M \in \{l,c\}$ (denoted as $\hat{\beta}^M_{j,i}$). The model accuracy can then be estimated as the mean absolute error of the estimated regression parameter $\hat{\beta}^M_j$, $j \in \{1,2\}$ for the linear model, $M = l$, and the circular model, $M = c$:

$$a_{M,j} = \frac{1}{m}\sum_{i=1}^{m} |\hat{\beta}^M_{j,i} - \beta_j| \tag{5}$$

The difference in accuracy for the ~~beta value as the efficiency of the model (i.e. lower values mean higher efficiency)~~ coefficient j between the circular and the linear model is shown in

$$\delta_{a,j} = a_{l,j} - a_{c,j} \tag{6}$$

Finally, the mean difference accuracy between the linear and the circular model is given by

$$\delta_a = \frac{\delta_{a,1} + \delta_{a,2}}{2} \tag{7}$$

The difference in precision for the coefficient j between the linear (l) and the circular model (c) is shown in

$$\delta_{p,j} = \mathrm{s}_{l,j} - \mathrm{s}_{c,j} \tag{8}$$

The mean difference precision between the linear and the circular model is given by

$$\delta_p = \frac{\delta_{p,1} + \delta_{p,2}}{2} \tag{9}$$

Where $\mathrm{s}_{M,j}$ is the sample standard deviation of the vector $(\hat{\beta}^M_{j,i})_i$, $M \in \{l,c\}$.

2.4 Analysis setup

The target variable $\mathrm{DOY}_{\mathrm{GPPmax}}$ is the day of the year when GPP reaches its maximum during the growing season. Given that different ecosystems present more than one growing season per year (e.g. semi-arid ecosystems) it is necessary to identify the number of growing seasons per year. To identify the number of growing seasons we apply a Fast Fourier Transformation (FFT)

(Cooley and Tukey, 1965) to the mean seasonal cycle of the GPP time series. The number of growing seasons is equal to the maximum absolute value of the first four FFT coefficients (excluding the first one). For each FLUXNET site, we reconstruct the GPP time series taking the real numbers of the inverse FFT. We use these reconstructed time series to calculate the expected mean timing of DOY_{GPPmax} and use this value as a template. To recover the real DOY_{GPPmax} from the original time series we define a window around the template of length inversely proportional to the number of cycles (180 days / Number of growing seasons). To increase the robustness of the analysis we identify the days with the 10 highest GPP values. These days are used in the block bootstrapping mentioned above. Finally, since most of the sites are located in the Northern Hemisphere we expect that in most cases DOY_{GPPmax} will be reached by middle of the calendar year.

To quantify the contribution of each climate variable, we count the number of sites per vegetation type where the regression coefficient is statistically significant. We perform a leave-one-out cross-validation per vegetation type to evaluate the predictive power of the circular regression using climate conditions. We only consider vegetation types with more than five sites. In this case the standardization of the climate variables is not applied. Finally, we use the mean of the optimum half-time parameter per vegetation type to weigh the climate conditions.

3 Results

Here, we first report results from simulated data to describe the performance of the circular regression approach compared to a linear model. Second, we compare the performance of circular and linear regression using empirical data. Third, we analyze the sensitivity of DOY_{GPPmax} across vegetation types and climate classes. Finally, we show the results of the predictive power of circular regression per vegetation type.

3.1 Circular vs. Linear Regression

Figure 3 (a,c) shows that for $\mu = 0$ (DOY_{GPPmax} at the beginning of the year) ~~and~~ circular regression has a higher accuracy and precision compared to the linear regression for the entire space of regression coefficient values, with a maximum difference in the order of 0.1 in terms of accuracy, and the order of 1 for precision. For $\mu = \pi$ (DOY_{GPPmax} mid-year) the ~~circular regression method is generally more efficient as it has a lower distance in case of β_1. For β_2 linear regression performs better than circular regression when the amount of data is higher than 100. Nevertheless, the differences between both regressions for β_2 are~~ linear model has a higher accuracy in most of the evaluated space with a maximum difference in the order of ~~0.2 while the differences for β_1 are~~ 0.001 compared with the circular regression. While, circular regression has a higher precision for most of the regression coefficients in the order of ~~0.5~~0.001. These results show that circular regression ~~produces more accurate results~~ has a higher precision to recover the original regression coefficients than linear regression ~~in terms of the coefficient estimation~~no matter the moment of the year. On the other hand, circular regression has a higher accuracy than linear model at the beginning of the year. While at mid-year when linear is better the differences are in the order of 0.001.

To illustrate the method in practice, we compare the circular and linear models using data from two sites: US-Ha1 (Northern Hemisphere, deciduous broadleaf forest), and AU-How (Southern Hemisphere, woody savanna). We relate the climate variables

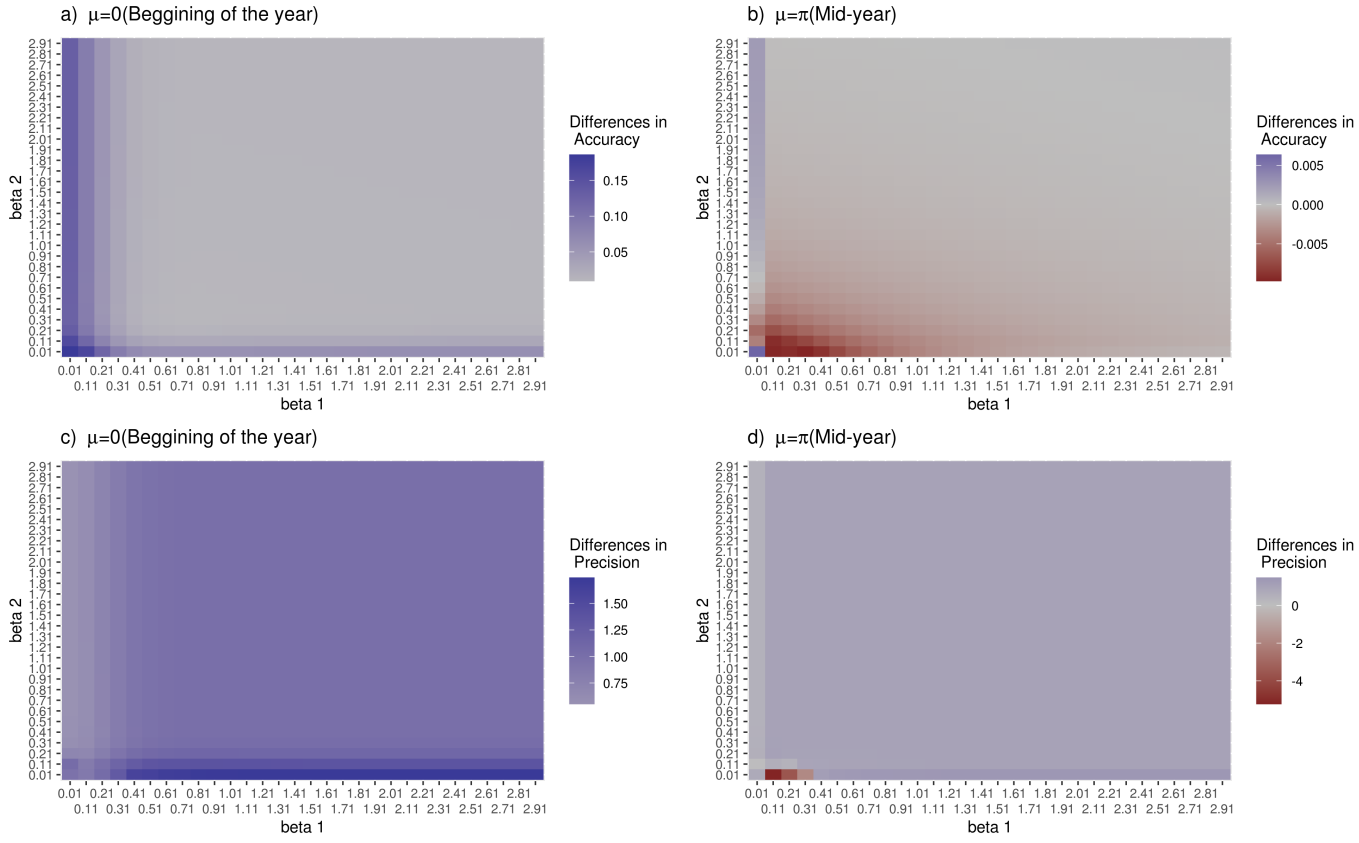

Figure 3. ~~Efficiency~~ Accuracy and precision of linear and circular regression models by recovering the original regression coefficients of a circular regression~~for different numbers of data (lower values mean higher efficiency)~~. ~~Upper~~ Left side: ~~$\mu = \pi$ (Maximum at mid-year).~~ ~~Bottom side~~ $\mu = 0$ (Maximum at the beginning of the year). ~~The effect is analyzed for each regression coefficient individually~~Right side $\mu = pi$ (Maximum at Mid-year). a. and ~~e~~b. correspond to the ~~regression coefficient β_1 and b~~differences in accuracy between the models. c. and d. correspond to the ~~regression coefficient β_2~~differences in the precision between the models. The blue color means better performance of the circular model compared with the linear model, and red color means higher performance of the linear model.

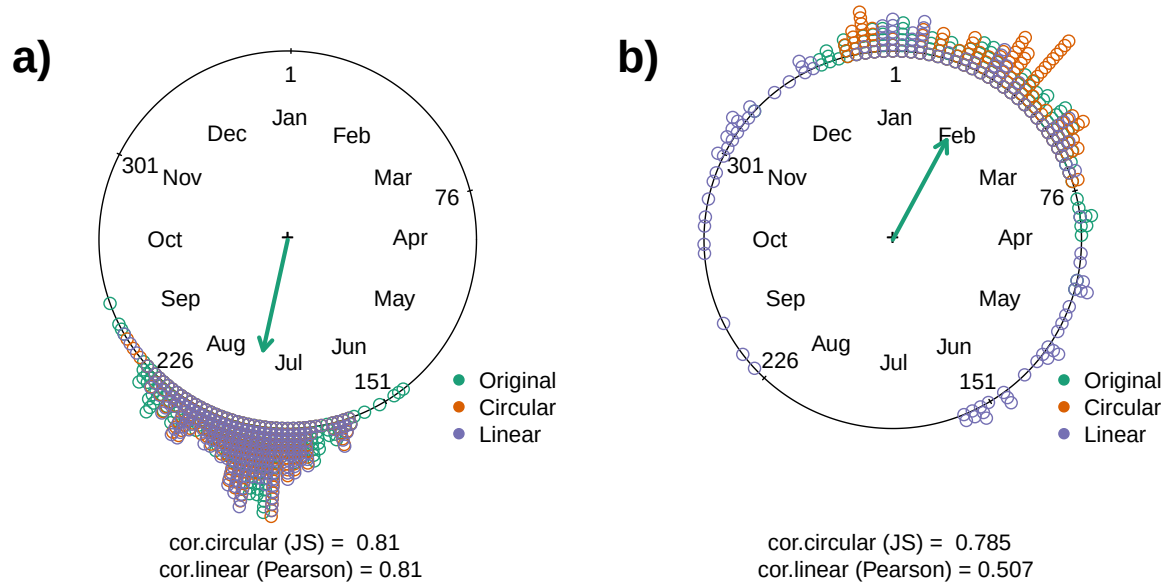

Figure 4. Correlation coefficient between the observed and predicted DOY_{GPPmax} using climatic variables. Two sites are presented: a. US-Ha1, and b. AU-How. The observed DOY_{GPPmax} (Green) is compared with the data retrieved using Circular (Orange) and Linear (Purple) regressions. Two correlation coefficients are used: Jammalamadaka-Sarna (JS) and Pearson product-moment (Pearson). In the circular plot the months and the day of the year (DOY) are also plotted every 75 days. The green arrow indicates the mean angular direction of the original data distribution.

with DOY_{GPPmax} (See methods) and reconstructed the DOY_{GPPmax} using the linear and circular regression models. We compare observed and predicted DOY_{GPPmax} using JS correlation for circular model and Pearson-Product Moment for linear model. For US-Ha1 both methods shows similar performance predicting DOY_{GPPmax} (Figure 4), while for AU-How, the circular model retrieves the original data better than the linear model explaining 30 % more of the variance. In the case when the DOY_{GPPmax} is reached at the beginning of the year, linear methods produce a strong bias that predicts the timing across the entire year (Figure 4,b).

3.2 Sensitivity of DOY_{GPPmax} to climate variables

From 52 sites analyzed in this study, only one site (ES-LJu) shows a bimodal growing seasons (see Supplement 1.2). As expected in most cases DOY_{GPPmax} occurs at the middle of the calendar year (Figure S6), reflecting the uneven site distribution in FLUXNET (Schimel et al., 2015). However some ecosystems in the Northern Hemisphere do reach DOY_{GPPmax} at the beginning of the year, these are Mediterranean sites such as, US-Var and ES-LJu. In general terms, most of the sites have a standard deviation between 10 [days] and 40 [days]. The maximal standard deviation is 46.9 [days] for AU-Tum site. A detailed table with the mean angular direction and standard deviation of DOY_{GPPmax} of each site is presented in section S1.2.

For half of the sites, the JS correlation coefficients are between 0.70 and 0.97 (Supplement 1, Figure S5) showing that the inter-annual variability of DOY_{GPPmax} is mainly explained by the cumulative effect of the climate variables. Nineteen sites have a JS coefficient less than 0.7 (DK-Sor, FI-Hyy, US-MMS, DK-ZaH, FR-Pue, US-UMB, AU-Tum, US-Ton, FR-LBr, US-Me2, IT-Lav, AT-Neu, DE-Gri, IT-MBo, IT-Ro2, US-Wkg, BR-Sa1, FR-Fon, CZ-wet). For ES-LJu the JS coefficient for the first growing season is 0.77 and 0.78 for the second one (Table S2).

Across all sites we find that air temperature, shortwave incoming radiation, and vapor pressure deficit appear as the dominant drivers worldwide in 43 sites (84 %, Supplement 3). Precipitation is the main driver for 5 sites (AU-How US-Ton ZA-Kru US-SRM US-Wkg, Supplement 3). Interestingly precipitation was the most important factor for all the woody savanna sites (Supplement 3). For three sites (DE-Gri, IT-Ro2, BRSa1) any climatic variable is significant. In terms of the sign of the coefficients, all the variables are predominantly negative (Table 1). This means that higher values of radiation, air temperature, VPD and precipitation lead to an earlier DOY_{GPPmax}. Individual sensitivities per site are shown in Supplement 3.

Table 1. Number of FLUXNET sites where each regression coefficient is statistically significant to explain the physio-phenology of GPPmax (DOY_{GPPmax}). The table is divided by the sign of the coefficient. The first column is coefficient for the dimensionality reduction between: Air temperature (Tair), Shortwave incoming radiation (SWin), and Vapor pressure deficit (VPD), the second column is the coefficient for Precipitation (Precip).

	Climatic variable	
Sign	Tair, SWin, VPD	Precip
(+)	8	2
(-)	38	14

The PCA between shortwave incoming radiation, air temperature and vapor pressure deficit has the highest frequency of significant corrrelation coefficients by number of sites for all the vegetation types with exception of Woody Savannas (WSA) where precipitation show to be more important for most sites than the dimensionality reduction between Tair, SWin, and VPD (Figure 5). For Closed Shrublands (CSH), and Savannas (SAV) both drivers have the same number of sites where the coefficients are statistically significant.

A special case to understand the sensitivity of DOY_{GPPmax} to climate variables is the site: “Llano de los Juanes” an open shrubland ecosysten in Spain (ES-LJu). It is the only clearly bimodal ecosystem in our study (Figure 6). In this case precipita-

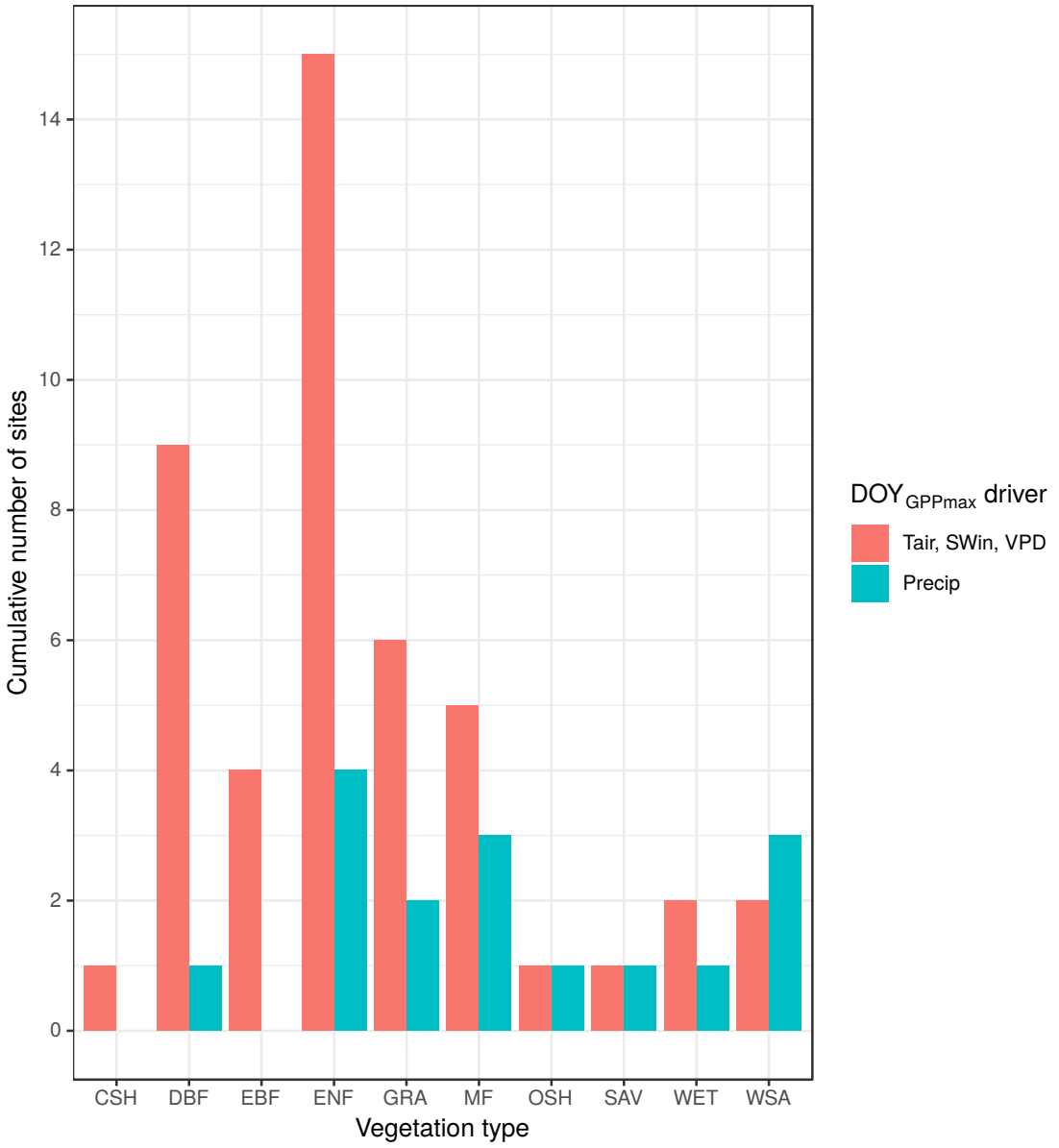

Figure 5. Contribution of each climate variable to explain the inter-annual variation of DOY_{GPPmax} per vegetation type. CSH: Closed Shrublands (n = 1), DBF: Deciduous Broadleaf Forest (n = 10), EBF: Evergreen Broadleaf Forest (n = 5), ENF: Evergreen Needleleaf Forest (n = 15), GRA: Grassland (n = 8), MF: Mixed Forest (n = 5), OSH: Open Shrublands (n = 1), SAV: Savannas (n = 1), WET: Permanent wetlands (n = 2), WSA: Woody Savannas (n = 3). Each bar shows the cumulative number of sites where each climate variables are statistically significant.

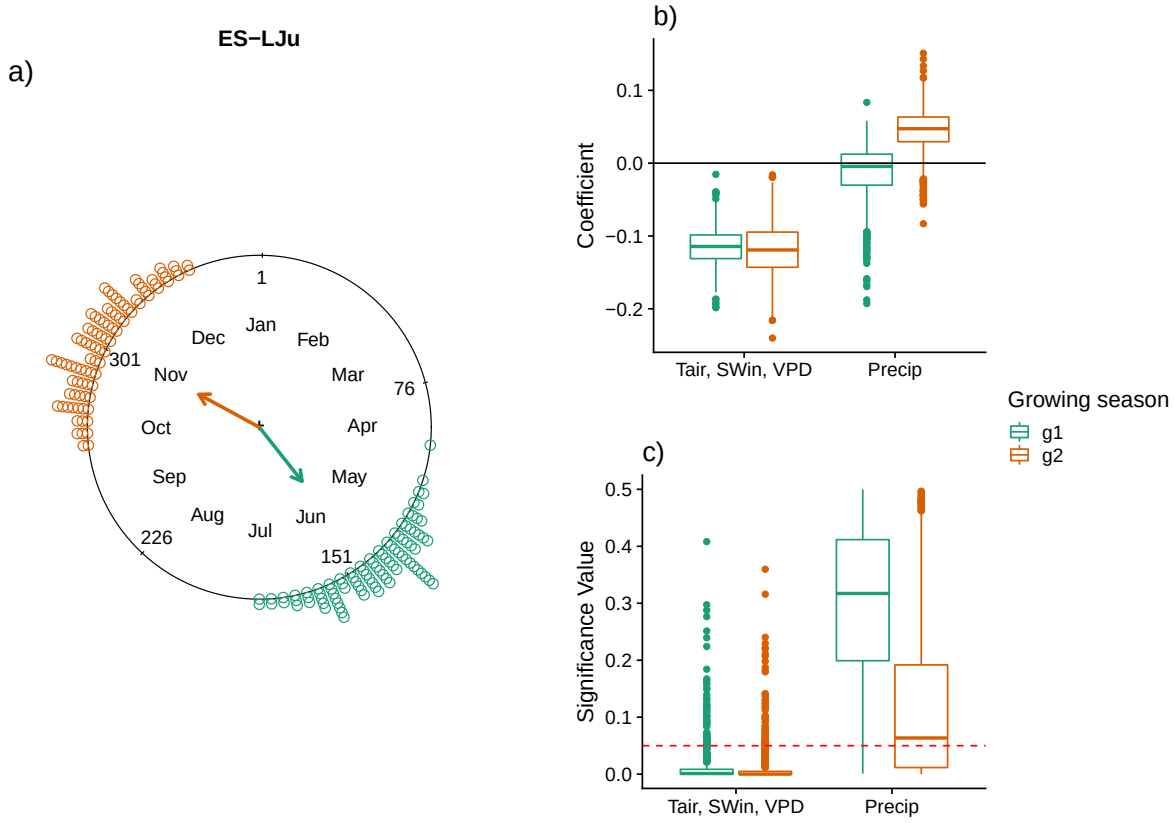

Figure 6. DOY_{GPPmax} sensitivity to different climate drivers in a Mediterranean ecosystem: "Llano de los Juanes", Spain (ES-Lju) with two growing seasons (green and orange). a) DOY_{GPPmax} distribution across the year. The arrows indicate the mean angular direction of the growing season. b) regression coefficients for each growing season and c) the significance values for each variable. The red line in c) represents a p-value of 0.05.

tion is not statistically significant. While the combination of Tair, SWin and VPD is significant for both seasons. Furthermore, in both growing seasons Tair, SWin and VPD have a negative coefficient.

The leave-one-site-out cross-validation for several vegetation types shows that the predictive power of the ~~prediction of the~~ model for GRA and EBF is -0.3 and -0.31 respectively. For DBF is 0.46 and for ENF is 0.4. While for MF the ~~power prediction~~ predictive power of the model is 0.88, respectively (Figure 7).

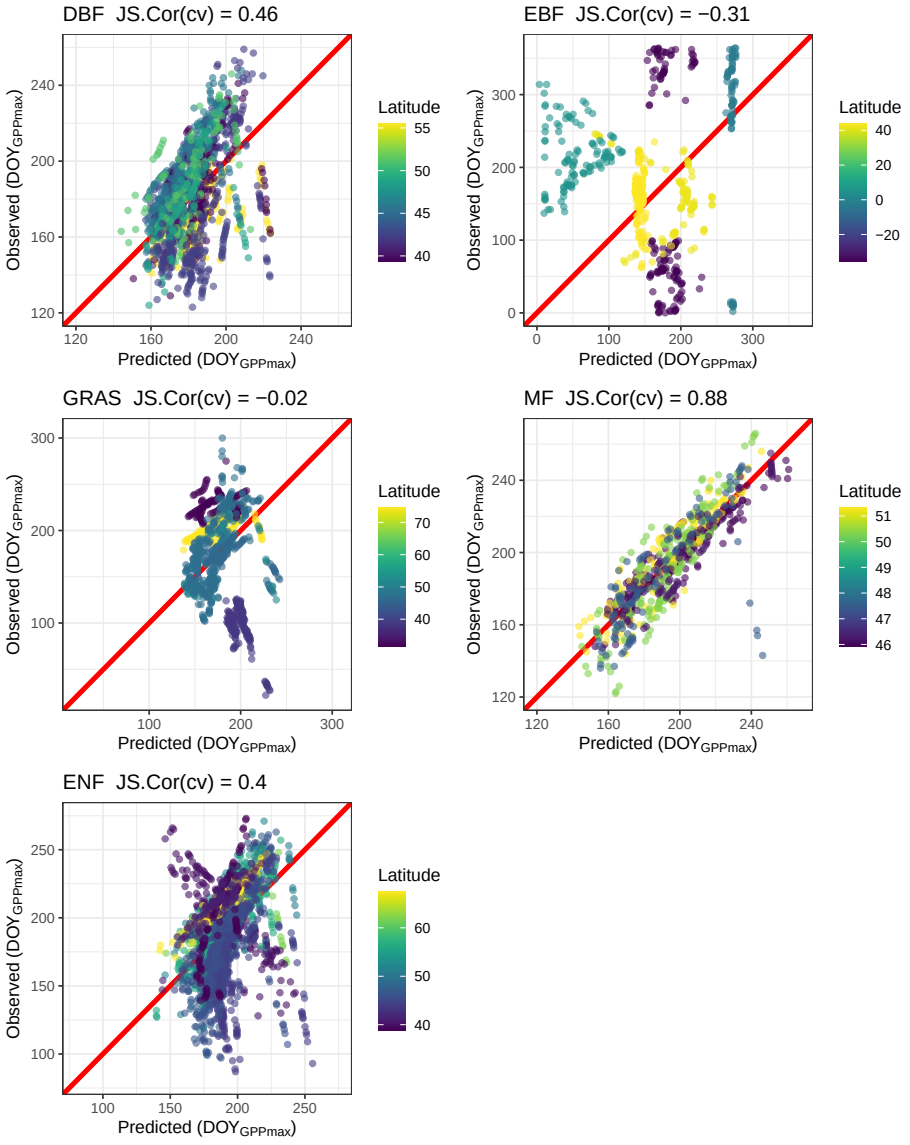

Figure 7. Cross validation of the circular regression model to predict DOY_{GPPmax} for different vegetation types using air temperature, shortwave incoming radiation, precipitation and vapor pressure deficit (see methods). Deciduous Broadleaf Forest (DBF). Evergreen Broadleaf Forest (EBF). Grassland (GRA). Mixed Forest (MF), and Evergreen Needleleaf Forest (ENF). For each ~~site~~ vegetation type the Jammalamadaka-Sarna (JS) correlation coefficient is shown in the title of each plot. The red line represents the perfect fit.~~The blue line shows the tendency of the data.~~

4 Discussion

4.1 Circular vs Linear regression

We explored whether circular regression is a suitable tool to analyze phenological events. Our results suggest that circular regressions can recover predefined coefficients in a set of simulations with higher accuracy and precision than linear regressions. Hence, we would generally suggest that circular regressions may be advantageous when the aim is analyzing the effect of climatic variables on phenological events. We did find, ~~however,~~ also cases where the classical linear regression may be either more robust or equally suitable e.g. when phenological events are reached close to the mid-year. In the overall view, however, we consider that circular regressions are to be preferred over linear regression for their conceptual capacity to analyze the physio-phenology of ecosystems regardless of the day of the year when an event of interest occurs. This allows us to analysing phenological studies at global scale regardless of geographic location or the distribution of the observations during the year.

~~Richardson et al. (2013) concluded that phenology models need to be improved as a prerequisite to extending the prediction capacity of global-scale models~~ Different phenological models have been developed ranging from empirical approaches (Richardson et al., 2013) to process models (Asse et al., 2020) over the last decades. As we demonstrate here, circular statistics ~~open new opportunities for this aim~~opens new opportunities to increase the robustness of phenological models allowing to analyze ecosystems across hemispheres within the same consistent framework. In fact, the results on phenological sensitivity of DOY_{GPPmax} ~~in this study~~ indicate the complexity of ecosystem responses to climate variability. ~~Indeed we considered our approach as a first step to implement~~ Our approach is a motivation towards integrating circular regressions into more complex statistical techniques like ~~decision~~ regression trees, Gaussian process, or artificial neural networks, targeting a circular response variable.

4.2 Sensitivity of DOY_{GPPmax} to climate variables

The geographical location of the FLUXNET 2015 sites represent an advantage to capture the DOY_{GPPmax} variability at global scale (Supplement 1, Figure S6). Most of the analyzed sites (47) are located in the Northern Hemisphere. Two sites (GF-Guy and BR-Sa1) are located in the tropical region and, 3 sites (ZA-Kru, AU-How, AU-Tum) in the Southern Hemisphere. However, because of the low number of sites reported in the tropical and southern region with more than seven years of data, our understanding about the DOY_{GPPmax} variability in these regions is still limited. Increasing the number of tropical and Southern Hemisphere sites should be considered a high-priority in the near future to complement our knowledge about the physio-phenological ecosystem state.

The high values of the JS correlation coefficients for most of the sites demonstrate that the inter-annual variability of DOY_{GPPmax} can be explained as the cumulative effect of the climate variables during the growing season. Sites where it was not possible to explain the variations of DOY_{GPPmax} with enough confidence level (JS correlation < 0.7) might require incorporating biotic variables (e.g. species composition (Peichl et al., 2018)) or soil properties information that can improve the ~~power prediction~~ predictive power of the model.

Our results suggest that there is no pattern between the DOY_{GPPmax} sensitivity across vegetation type or climate classes (Sect. Figure S1.7). In other words, the DOY_{GPPmax} sensitivity is site-specific, probably produced by the unique combination of biotic (e.g. species composition, species phenology, species interaction, and phenotypic plasticity) factors that are not evaluated in our study. Several studies that focused on ecosystem phenology suggest that species composition play a fundamental role in ecosystem physio-phenology of the CO_2 uptake (Gonsamo et al., 2017; Peichl et al., 2018).

While there is no clear relationship between the DOY_{GPPmax} sensitivity and the vegetation type, we find a predominant role of the combined effects of shortwave incoming radiation (SWin), air temperature (Tair) and vapor pressure deficit (VPD) at the global scale on the DOY_{GPPmax} inter-annual variability, where for most of the sites these variables have a negative regression coefficient. This means, that if the SWin, Tair, and VPD increase during the growing season the DOY_{GPPmax} will be reached earlier. This effect can be a consequence of DOY_{GPPmax} being reached at the same time as SWin and Tair are maximum.

On a global scale our analysis shows that the combination of air temperature, short-wave incoming radiation and vapour pressure deficit has a negative sign as well as precipitation. This means that if these variables increase during the growing season, the GPPmax will be reached earlier. Our results are similar to those obtained by Wang and Wu (2019) were the authors conclude that an increase in the temperature produces an earlier DOY_{GPPmax}. This phenomenon is likely explained by the leaf-out advancing during spring. Nevertheless, there is still no consensus on whether the increase in temperature will produce an earlier end to the growing season. Several studies demonstrated for different vegetation types that when temperature increases, spring onset is earlier and autumn senescence is later (Christensen et al., 2007; Linkosalo et al., 2009; Migliavacca et al., 2012; Morin et al., 2010; Post and Forchhammer, 2008), increasing the length of the growing season and the amount of CO_2 that is uptake by ecosystems (Richardson et al., 2013).

Ecosystems with two growing seasons per year represent a very interesting case of the effect of climate drivers on DOY_{GPPmax} across different growing seasons. In Llano de los Juanes, Spain (ES-LJu, Figure 6) DOY_{GPPmax} is reached in the first growing season when the rainy season is finishing, while in the second growing season DOY_{GPPmax} is reached in the middle of the rainy season (Data not shown). The effect of short-wave incoming radiation, temperature and vapor pressure deficit for both growing seasons is negative suggesting that if we increase these variables during the period before, the DOY_{GPPmax} will happen earlier.

Phenology in Mediterranean ecosystems is mainly controlled by water availability (Kramer et al., 2000; Luo et al., 2018; Peñuelas et al., 2009). However, our results suggest that DOY_{GPPmax} is mainly sensitive to SWin, Tair, and VPD. This result agrees with the analysis performed by Gordo and Sanz (2005) were the authors evaluated the phenological sensitivity of Mediterranean ecosystem to temperature and precipitation, and they concluded that temperature was the most important driver. Although water is a limiting factor in Mediterranean ecosystems, its influence on plant physiology and plant phenology can be completely different. In terms of physiology the GPPmax value can decrease but in terms of phenology DOY_{GPPmax} can be still the same.

Complex interactions between climate variables and phenological response and the interspecificity of the sensitivity at site level explain in part the poor ~~power prediction~~ predictive power of the model for grasslands, Evergreen Broadleaf Forest, Evergreen Needleleaf Forest, and Deciduous Broadleaf Forests in the cross validation analysis (Figure 7). However, the ~~power prediction~~ predictive power for Mixed Forest is high, also when the distribution of the latitudinal gradient is not the same

for all the sites. These results reflect that circular regression model can be extrapolated from different sites, to predict the DOY_{GPPmax} inter-annual variability. This advantage could be a way to solve the common critic that phenological models can not be extrapolated generating only ad-hoc hypothesis (Richardson et al., 2013).

5 Conclusions

In this study we explore the potential of "circular regressions" to explain the physio-phenology of maximal CO_2 uptake rates. We conclude that 1) shortwave incoming radiation, temperature and vapor pressure deficit are the main drivers of the timing of maximal CO_2 uptake at global scale; precipitation only play a secondary role with the exception of woody savannas where the most important variable is precipitation. 2) Although the sensitivity of the DOY_{GPPmax} to the climate drivers is site specific, it is possible to extrapolate the circular regression model for different sites with the same vegetation type and similar latitudes. Finally, we demonstrated using simulated and empirical data, that circular regression produces more accurate results than linear regression, in particular in cases when data needs to be explored across hemispheres.

Acknowledgements. We thank the reviewers for their helpful suggestions and Guido Kraemer for his help with the mathematical notation. This project has received funding from the European Union's Horizon 2020 research and innovation programme via the Trustee project under the Marie Skłodowska-Curie grant agreement No 721995. This work used eddy covariance data acquired and shared by the FLUXNET community, including these networks: AmeriFlux, AfriFlux, AsiaFlux, CarboAfrica, CarboEuropeIP, CarboItaly, CarboMont, ChinaFlux, Fluxnet-Canada, GreenGrass, ICOS, KoFlux, LBA, NECC, OzFlux-TERN, TCOS-Siberia, and USCCC. The ERA-Interim reanalysis data are provided by ECMWF and processed by LSCE. The FLUXNET eddy covariance data processing and harmonization was carried out by the European Fluxes Database Cluster, AmeriFlux Management Project, and Fluxdata project of FLUXNET, with the support of CDIAC and ICOS Ecosystem Thematic Center, and the OzFlux, ChinaFlux and AsiaFlux offices.

Appendix A: FLUXNET Sites

Table A1: FLUXNET sites used in our study. We report the name of the sites, time period used for the analysis, the climate class of each site following the Köppen-Geiger classification: Tropical monsoon climate (Am), Tropical savanna climate (Aw), Cold semi-arid climates (BSk), Humid subtropical climate (Cfa), Oceanic climate (Cfb), Hot-summer mediterranean climate (Csa), Warm-summer mediterranean climate (Csb), Humid subtropical climate (Cwa), humid continental climate (Dfb), Subarctic climate (Dfc, Dsc), and Tundra climate (ET). We also report the Vegetation type of the sites: Closed Shrublands (CSH), Deciduous Broadleaf Forests (DBF), Evergreen Broadleaf Forest (EBF), Evergreen Needleleaf Forests (ENF), Grasslands (GRA), Mixed Forests (MF), Open Shrublands (OSH), Savannas (SAV), Permanent Wetlands (WET), Woody Savannas (WSA).

Site name	Köppen-Geiger class	Vegetation type	Period	N. years analyzed	Citation	Data DOI
AT-Neu	Dfc	GRA	2002:2012	11	(Wohlfahrt et al., 2008)	10.18140/FLX/1440121
AU-How	Aw	WSA	2002:2014	13	(Beringer et al., 2007)	10.18140/FLX/1440125
AU-Tum	Cfb	EBF	2001:2014	14	(Leuning et al., 2005)	10.18140/FLX/1440126
BE-Bra	Cfb	MF	1999:2002, 2004:2014	15	(Carrara et al., 2004)	10.18140/FLX/1440128
BE-Vie	Cfb	MF	1997:2014	18	(Aubinet et al., 2001)	10.18140/FLX/1440130
BR-Sa1	Am	EBF	2002:2005, 2009:2011	7	(Saleska et al., 2003)	10.18140/FLX/1440032
CA-Man	Dfc	ENF	1994:1996, 1998:2003	12	(Brooks et al., 1997)	10.18140/FLX/1440035
CH-Cha	Cfb	GRA	2005:2014	10	(Merbold et al., 2014)	10.18140/FLX/1440131
CH-Dav	ET	ENF	1997:2014	18	(Zielis et al., 2014)	10.18140/FLX/1440178
CH-Fru	Cfb	GRA	2005:2014	10	(Imer et al., 2013)	10.18140/FLX/1440133
CH-Lae	Cfb	MF	2004:2014	11	(Etzold et al., 2011)	10.18140/FLX/1440134
CZ-wet	Cfb	WET	2006:2014	9	(Dušek et al., 2012)	10.18140/FLX/1440145
DE-Gri	Cfb	GRA	2004:2014	11	(Prescher et al., 2010)	10.18140/FLX/1440147
DE-Hai	Cfb	DBF	2000:2012	13	(Knohl et al., 2003)	10.18140/FLX/1440148

DE-Tha	Cfb	ENF	1996:2014	19	(GrüNwald and Bernhofer, 2007)	10.18140/FLX/1440152
DK-Sor	Cfb	DBF	1996:2014	19	(Pilegaard et al., 2011)	10.18140/FLX/1440155
DK-ZaH	ET	GRA	2000:2010, 2012:2014	14	(Lund et al., 2012)	10.18140/FLX/1440224
ES-LJu	Csa	OSH	2005:2013	9	(Serrano-Ortiz et al., 2009)	10.18140/FLX/1440226
FI-Hyy	Dfc	ENF	1996:2014	19	(Suni et al., 2003)	10.18140/FLX/1440158
FI-Sod	Dfc	ENF	2001:2014	14	(Thum et al., 2007)	10.18140/FLX/1440160
FR-Fon	Cfb	DBF	2005:2014	10	(Delpierre et al., 2016)	10.18140/FLX/1440161
FR-LBr	Cfb	ENF	1996:2008	13	(Berbigier et al., 2001)	10.18140/FLX/1440163
FR-Pue	Csa	EBF	2000:2015	15	(Rambal et al., 2004)	10.18140/FLX/1440164
GF-Guy	Am	EBF	2004:2014	11	(Bonal et al., 2008)	10.18140/FLX/1440165
IT-Col	Csa	DBF	1996:2014	19	(Valentini et al., 1996)	10.18140/FLX/1440167
IT-Cpz	Csa	EBF	2000:2008	9	(Garbulsky et al., 2008)	10.18140/FLX/1440168
IT-Lav	Cfb	ENF	2003:2014	12	(Marcolla et al., 2003)	10.18140/FLX/1440169
IT-MBo	Dfb	GRA	2003:2013	11	(Marcolla et al., 2011)	10.18140/FLX/1440170
IT-Noe	Csa	CSH	2004:2014	11	(Marras et al., 2011)	10.18140/FLX/1440171
IT-Ren	Dfc	ENF	1999, 2002:2003, 2005:2013	12	(Montagnani et al., 2009)	10.18140/FLX/1440173
IT-Ro1	Csa	DBF	2001:2008	8	(Rey et al., 2002)	10.18140/FLX/1440174
IT-Ro2	Csa	DBF	2002:2008, 2010:2012	10	(Tedeschi et al., 2006)	10.18140/FLX/1440175
IT-SRo	Csa	ENF	1999:2012	14	(Chiesi et al., 2005)	10.18140/FLX/1440176
NL-Loo	Cfb	ENF	1996:2014	18	(Moors, 2012)	10.18140/FLX/1440178

RU-Cok	Dsc	OSH	2003:2013	11	(Molen et al., 2007)	10.18140/FLX/1440182
RU-Fyo	Dfb	ENF	1998:2014	17	(Kurbatova et al., 2008)	10.18140/FLX/1440183
US-Blo	Csa	ENF	1997:2007	11	(Baker et al., 1999)	10.18140/FLX/1440068
US-GLE	Dfc	ENF	2005:2014	10	(McDowell et al., 2000)	10.18140/FLX/1440069
US-Ha1	Dfb	DBF	1992:2012	21	(Urbanski et al., 2007)	10.18140/FLX/1440071
US-Los	Dfb	WET	2001:2008, 2010, 2014	10	(Davis et al., 2003)	10.18140/FLX/1440076
US-Me2	Csb	ENF	2002:2014	13	(Treuhaft et al., 2004)	10.18140/FLX/1440079
US-MMS	Cfa	DBF	1999:2014	16	(Schmid et al., 2000)	10.18140/FLX/1440083
US-NR1	Dfc	ENF	1999:2014	16	(Monson et al., 2002)	10.18140/FLX/1440087
US-PFa	Dfb	MF	1996:2014	19	(Berger et al., 2001)	10.18140/FLX/1440089
US-SRM	BSk	WSA	2004:2014	11	(Scott et al., 2008)	10.18140/FLX/1440090
US-Syv	Dfb	MF	2001:2007, 2012:2014	10	(Desai et al., 2005)	10.18140/FLX/1440091
US-Ton	Csa	WSA	2001:2014	14	(Xu and Baldocchi, 2003)	10.18140/FLX/1440092
US-UMB	Dfb	DBF	2000:2014	15	(Curtis et al., 2002)	10.18140/FLX/1440093
US-Var	Csa	GRA	2001:2014	14	(Xu and Baldocchi, 2004)	10.18140/FLX/1440094
US-WCr	Dfb	DBF	1999:2006, 2011:2014	12	(Curtis et al., 2002)	10.18140/FLX/1440095
US-Wkg	BSk	GRA	2004:2014	11	(Emmerich, 2003)	10.18140/FLX/1440096
ZA-Kru	Cwa	SAV	2000:2005, 2007:2013	13	(Archibald et al., 2009)	10.18140/FLX/1440188

References

Agostinelli, C. and Lund, U.: R package circular: Circular Statistics (version 0.4-93), CA: Department of Environmental Sciences, Informatics and Statistics, Ca' Foscari University, Venice, Italy. UL: Department of Statistics, California Polytechnic State University, San Luis Obispo, California, USA, https://r-forge.r-project.org/projects/circular/, 2017.

Archibald, S. A., Kirton, A., Merwe, M. R. v. d., Scholes, R. J., Williams, C. A., and Hanan, N.: Drivers of inter-annual variability in Net Ecosystem Exchange in a semi-arid savanna ecosystem, South Africa, Biogeosciences, 6, 251–266, https://doi.org/https://doi.org/10.5194/bg-6-251-2009, https://www.biogeosciences.net/6/251/2009/, publisher: Copernicus GmbH, 2009.

Asse, D., Randin, C. F., Bonhomme, M., Delestrade, A., and Chuine, I.: Process-based models outcompete correlative models in projecting spring phenology of trees in a future warmer climate, Agricultural and Forest Meteorology, 285-286, 107 931, https://doi.org/10.1016/j.agrformet.2020.107931, http://www.sciencedirect.com/science/article/pii/S0168192320300332, 2020.

Aubinet, M., Chermanne, B., Vandenhaute, M., Longdoz, B., Yernaux, M., and Laitat, E.: Long term carbon dioxide exchange above a mixed forest in the Belgian Ardennes, Agricultural and Forest Meteorology, 108, 293–315, https://doi.org/10.1016/S0168-1923(01)00244-1, http://www.sciencedirect.com/science/article/pii/S0168192301002441, 2001.

Aubinet, M., Vesala, T., and Papale, D., eds.: Eddy Covariance: A Practical Guide to Measurement and Data Analysis, Springer Atmospheric Sciences, Springer Netherlands, https://www.springer.com/de/book/9789400723504, 2012.

Baker, B., Guenther, A., Greenberg, J., Goldstein, A., and Fall, R.: Canopy fluxes of 2-methyl-3-buten-2-ol over a ponderosa pine forest by relaxed eddy accumulation: Field data and model comparison, Journal of Geophysical Research: Atmospheres, 104, 26 107–26 114, https://doi.org/10.1029/1999JD900749, https://agupubs.onlinelibrary.wiley.com/doi/abs/10.1029/1999JD900749, _eprint: https://agupubs.onlinelibrary.wiley.com/doi/pdf/10.1029/1999JD900749, 1999.

Baldocchi, D., Falge, E., Gu, L., Olson, R., Hollinger, D., Running, S., Anthoni, P., Bernhofer, C., Davis, K., Evans, R., Fuentes, J., Goldstein, A., Katul, G., Law, B., Lee, X., Malhi, Y., Meyers, T., Munger, W., Oechel, W., Paw U, K. T., Pilegaard, K., Schmid, H. P., Valentini, R., Verma, S., Vesala, T., Wilson, K., and Wofsy, S.: FLUXNET: A New Tool to Study the Temporal and Spatial Variability of Ecosystem-Scale Carbon Dioxide, Water Vapor, and Energy Flux Densities, Bulletin of the American Meteorological Society, 82, 2415–2434, https://doi.org/10.1175/1520-0477(2001)082<2415:FANTTS>2.3.CO;2, https://journals.ametsoc.org/doi/abs/10.1175/1520-0477(2001)082%3C2415:FANTTS%3E2.3.CO;2, publisher: American Meteorological Society, 2001.

Baldocchi, D. D.: How eddy covariance flux measurements have contributed to our understanding of Global Change Biology, Global Change Biology, 26, 242–260, https://doi.org/10.1111/gcb.14807, https://onlinelibrary.wiley.com/doi/abs/10.1111/gcb.14807, _eprint: https://onlinelibrary.wiley.com/doi/pdf/10.1111/gcb.14807, 2020.

Bauerle, W. L., Oren, R., Way, D. A., Qian, S. S., Stoy, P. C., Thornton, P. E., Bowden, J. D., Hoffman, F. M., and Reynolds, R. F.: Photoperiodic regulation of the seasonal pattern of photosynthetic capacity and the implications for carbon cycling, Proceedings of the National Academy of Sciences, 109, 8612–8617, https://doi.org/10.1073/pnas.1119131109, https://www.pnas.org/content/109/22/8612, publisher: National Academy of Sciences Section: Biological Sciences, 2012.

Berbigier, P., Bonnefond, J.-M., and Mellmann, P.: CO2 and water vapour fluxes for 2 years above Euroflux forest site, Agricultural and Forest Meteorology, 108, 183–197, https://doi.org/10.1016/S0168-1923(01)00240-4, http://www.sciencedirect.com/science/article/pii/S0168192301002404, 2001.

Berger, B. W., Davis, K. J., Yi, C., Bakwin, P. S., and Zhao, C. L.: Long-Term Carbon Dioxide Fluxes from a Very Tall Tower in a Northern Forest: Flux Measurement Methodology, Journal of Atmospheric and Oceanic Technology, 18, 529–

542, https://doi.org/10.1175/1520-0426(2001)018<0529:LTCDFF>2.0.CO;2, https://journals.ametsoc.org/doi/full/10.1175/1520-0426%282001%29018%3C0529%3ALTCDFF%3E2.0.CO%3B2, publisher: American Meteorological Society, 2001.

Beringer, J., Hutley, L. B., Tapper, N. J., and Cernusak, L. A.: Savanna fires and their impact on net ecosystem productivity in North Australia, Global Change Biology, 13, 990–1004, https://doi.org/10.1111/j.1365-2486.2007.01334.x, https://onlinelibrary.wiley.com/doi/abs/10.1111/j.1365-2486.2007.01334.x, _eprint: https://onlinelibrary.wiley.com/doi/pdf/10.1111/j.1365-2486.2007.01334.x, 2007.

Beyene, M. T., Jain, S., and Gupta, R. C.: Linear-Circular Statistical Modeling of Lake Ice-Out Dates, Water Resources Research, 54, 7841–7858, https://doi.org/10.1029/2017WR021731, https://agupubs.onlinelibrary.wiley.com/doi/abs/10.1029/2017WR021731, _eprint: https://agupubs.onlinelibrary.wiley.com/doi/pdf/10.1029/2017WR021731, 2018.

Bonal, D., Bosc, A., Ponton, S., Goret, J.-Y., Burban, B., Gross, P., Bonnefond, J.-M., Elbers, J., Longdoz, B., Epron, D., Guehl, J.-M., and Granier, A.: Impact of severe dry season on net ecosystem exchange in the Neotropical rainforest of French Guiana, Global Change Biology, 14, 1917–1933, https://doi.org/10.1111/j.1365-2486.2008.01610.x, https://onlinelibrary.wiley.com/doi/abs/10.1111/j.1365-2486.2008.01610.x, _eprint: https://onlinelibrary.wiley.com/doi/pdf/10.1111/j.1365-2486.2008.01610.x, 2008.

Brooks, J. R., Flanagan, L. B., Varney, G. T., and Ehleringer, J. R.: Vertical gradients in photosynthetic gas exchange characteristics and refixation of respired CO2 within boreal forest canopies, Tree Physiology, 17, 1–12, https://doi.org/10.1093/treephys/17.1.1, https://academic.oup.com/treephys/article/17/1/1/1640508, publisher: Oxford Academic, 1997.

Carrara, A., Janssens, I. A., Curiel Yuste, J., and Ceulemans, R.: Seasonal changes in photosynthesis, respiration and NEE of a mixed temperate forest, Agricultural and Forest Meteorology, 126, 15–31, https://doi.org/10.1016/j.agrformet.2004.05.002, http://www.sciencedirect.com/science/article/pii/S0168192304001145, 2004.

Chiesi, M., Maselli, F., Bindi, M., Fibbi, L., Cherubini, P., Arlotta, E., Tirone, G., Matteucci, G., and Seufert, G.: Modelling carbon budget of Mediterranean forests using ground and remote sensing measurements, Agricultural and Forest Meteorology, 135, 22–34, https://doi.org/10.1016/j.agrformet.2005.09.011, http://www.sciencedirect.com/science/article/pii/S0168192305002108, 2005.

Christensen, J., Hewitson, B., Busuioc, A., Chen, A., Gao, X., Held, I., Jones, R., Kolli, R., Kwon, W.-T., Laprise, R., Rueda, V., Mearns, L., Menéndez, C., Räisänen, J., Rinke, A., Sarr, A., and Whetton, P.: Regional climate projections. Climate change 2007: The physical science basis, Contribution of Working Group I to the Fourth Assessment Report of the Intergovernmental Panel on Climate Change, pp. 847–940, 2007.

Cooley, J. W. and Tukey, J. W.: An Algorithm for the Machine Calculation of Complex Fourier Series, Mathematics of Computation, 19, 297–301, https://doi.org/10.2307/2003354, https://www.jstor.org/stable/2003354, 1965.

Curtis, P. S., Hanson, P. J., Bolstad, P., Barford, C., Randolph, J. C., Schmid, H. P., and Wilson, K. B.: Biometric and eddy-covariance based estimates of annual carbon storage in five eastern North American deciduous forests, Agricultural and Forest Meteorology, 113, 3–19, https://doi.org/10.1016/S0168-1923(02)00099-0, http://www.sciencedirect.com/science/article/pii/S0168192302000990, tex.ids: curtis_biometric_2002, 2002.

Davis, K. J., Bakwin, P. S., Yi, C., Berger, B. W., Zhao, C., Teclaw, R. M., and Isebrands, J. G.: The annual cycles of CO2 and H2O exchange over a northern mixed forest as observed from a very tall tower, Global Change Biology, 9, 1278–1293, https://doi.org/10.1046/j.1365-2486.2003.00672.x, https://onlinelibrary.wiley.com/doi/abs/10.1046/j.1365-2486.2003.00672.x, _eprint: https://onlinelibrary.wiley.com/doi/pdf/10.1046/j.1365-2486.2003.00672.x tex.ids: davis_annual_2003, 2003.

Delpierre, N., Berveiller, D., Granda, E., and Dufrêne, E.: Wood phenology, not carbon input, controls the interannual variability of wood growth in a temperate oak forest, New Phytologist, 210, 459–470, https://doi.org/10.1111/nph.13771, https://nph.onlinelibrary.wiley.com/doi/abs/10.1111/nph.13771, _eprint: https://nph.onlinelibrary.wiley.com/doi/pdf/10.1111/nph.13771 tex.ids: delpierre_wood_2016, 2016.

Desai, A. R., Bolstad, P. V., Cook, B. D., Davis, K. J., and Carey, E. V.: Comparing net ecosystem exchange of carbon dioxide between an old-growth and mature forest in the upper Midwest, USA, Agricultural and Forest Meteorology, 128, 33–55, https://doi.org/10.1016/j.agrformet.2004.09.005, http://www.sciencedirect.com/science/article/pii/S0168192304002369, tex.ids: desai_comparing_2005, 2005.

Dušek, J., Čížková, H., Stellner, S., Czerný, R., and Květ, J.: Fluctuating water table affects gross ecosystem production and gross radiation use efficiency in a sedge-grass marsh, Hydrobiologia, 692, 57–66, https://doi.org/10.1007/s10750-012-0998-z, https://doi.org/10.1007/s10750-012-0998-z, tex.ids: dusek_fluctuating_2012, 2012.

Emmerich, W. E.: Carbon dioxide fluxes in a semiarid environment with high carbonate soils, Agricultural and Forest Meteorology, 116, 91–102, https://doi.org/10.1016/S0168-1923(02)00231-9, http://www.sciencedirect.com/science/article/pii/S0168192302002319, tex.ids: emmerich_carbon_2003, 2003.

Etzold, S., Ruehr, N. K., Zweifel, R., Dobbertin, M., Zingg, A., Pluess, P., Häsler, R., Eugster, W., and Buchmann, N.: The Carbon Balance of Two Contrasting Mountain Forest Ecosystems in Switzerland: Similar Annual Trends, but Seasonal Differences, Ecosystems, 14, 1289–1309, https://doi.org/10.1007/s10021-011-9481-3, https://doi.org/10.1007/s10021-011-9481-3, tex.ids: etzold_carbon_2011, 2011.

Fisher, N. I.: Statistical Analysis of Circular Data, Cambridge University Press, google-Books-ID: wGPj3EoFdJwC, 1995.

Fisher, N. I. and Lee, A. J.: Regression Models for an Angular Response, Biometrics, 48, 665–677, https://doi.org/10.2307/2532334, https://www.jstor.org/stable/2532334, publisher: [Wiley, International Biometric Society], 1992.

Garbulsky, M. F., Peñuelas, J., Papale, D., and Filella, I.: Remote estimation of carbon dioxide uptake by a Mediterranean forest, Global Change Biology, 14, 2860–2867, https://doi.org/10.1111/j.1365-2486.2008.01684.x, https://onlinelibrary.wiley.com/doi/abs/10.1111/j.1365-2486.2008.01684.x, 2008.

Gonsamo, A., D'Odorico, P., Chen, J. M., Wu, C., and Buchmann, N.: Changes in vegetation phenology are not reflected in atmospheric CO2 and 13C/12C seasonality, Global Change Biology, 23, 4029–4044, https://doi.org/10.1111/gcb.13646, https://onlinelibrary.wiley.com/doi/abs/10.1111/gcb.13646, 2017.

Gordo, O. and Sanz, J. J.: Phenology and climate change: a long-term study in a Mediterranean locality, Oecologia, 146, 484–495, https://doi.org/10.1007/s00442-005-0240-z, https://doi.org/10.1007/s00442-005-0240-z, 2005.

Green, P. J.: Iteratively Reweighted Least Squares for Maximum Likelihood Estimation, and some Robust and Resistant Alternatives, Journal of the Royal Statistical Society. Series B (Methodological), 46, 149–192, https://www.jstor.org/stable/2345503, 1984.

GrüNwald, T. and Bernhofer, C.: A decade of carbon, water and energy flux measurements of an old spruce forest at the Anchor Station Tharandt, Tellus B: Chemical and Physical Meteorology, 59, 387–396, https://doi.org/10.1111/j.1600-0889.2007.00259.x, https://doi.org/10.1111/j.1600-0889.2007.00259.x, 2007.

Hastie, T., Tibshirani, R., and Friedman, J. H.: The elements of statistical learning: data mining, inference, and prediction, Springer series in statistics, Springer, New York, NY, 2nd ed edn., 2009.

Imer, D., Merbold, L., Eugster, W., and Buchmann, N.: Temporal and spatial variations of soil CO_2, CH_4 and N_2O fluxes at three differently managed grasslands, Biogeosciences, 10, 5931–5945, https://doi.org/https://doi.org/10.5194/bg-10-5931-2013, https://www.biogeosciences.net/10/5931/2013/, publisher: Copernicus GmbH, 2013.

Jammalamadaka, S. R. and Sarma, Y.: A correlation coefficient for angular variables, Statistical theory and data analysis II, pp. 349–364, tex.publisher: Amsterdam North-Holland, 1988.

Knohl, A., Schulze, E.-D., Kolle, O., and Buchmann, N.: Large carbon uptake by an unmanaged 250-year-old deciduous forest in Central Germany, Agricultural and Forest Meteorology, 118, 151–167, https://doi.org/10.1016/S0168-1923(03)00115-1, http://www.sciencedirect.com/science/article/pii/S0168192303001151, 2003.

Kramer, K., Leinonen, I., and Loustau, D.: The importance of phenology for the evaluation of impact of climate change on growth of boreal, temperate and Mediterranean forests ecosystems: an overview, International Journal of Biometeorology, 44, 67–75, https://doi.org/10.1007/s004840000066, https://doi.org/10.1007/s004840000066, 2000.

Kurbatova, J., Li, C., Varlagin, A., Xiao, X., and Vygodskaya, N.: Modeling carbon dynamics in two adjacent spruce forests with different soil conditions in Russia, Biogeosciences, 5, 969–980, https://doi.org/https://doi.org/10.5194/bg-5-969-2008, https://www.biogeosciences.net/5/969/2008/, 2008.

Leuning, R., Cleugh, H. A., Zegelin, S. J., and Hughes, D.: Carbon and water fluxes over a temperate Eucalyptus forest and a tropical wet/dry savanna in Australia: measurements and comparison with MODIS remote sensing estimates, Agricultural and Forest Meteorology, 129, 151–173, https://doi.org/https://doi.org/10.1016/j.agrformet.2004.12.004, http://www.sciencedirect.com/science/article/pii/S0168192305000079, 2005.

Lieth, H., ed.: Phenology and Seasonality Modeling, Ecological Studies, Springer-Verlag, Berlin Heidelberg, https://www.springer.com/gp/book/9783642518652, citation Key Alias: lieth_phenology_1974, 1974.

Linkosalo, T., Häkkinen, R., Terhivuo, J., Tuomenvirta, H., and Hari, P.: The time series of flowering and leaf bud burst of boreal trees (1846–2005) support the direct temperature observations of climatic warming, Agricultural and Forest Meteorology, 149, 453–461, https://doi.org/10.1016/j.agrformet.2008.09.006, http://www.sciencedirect.com/science/article/pii/S0168192308002530, 2009.

Liu, Y., Schwalm, C. R., Samuels-Crow, K. E., and Ogle, K.: Ecological memory of daily carbon exchange across the globe and its importance in drylands, Ecology Letters, 0, https://doi.org/10.1111/ele.13363, https://onlinelibrary.wiley.com/doi/abs/10.1111/ele.13363, 2019.

Lund, M., Falk, J. M., Friborg, T., Mbufong, H. N., Sigsgaard, C., Soegaard, H., and Tamstorf, M. P.: Trends in CO2 exchange in a high Arctic tundra heath, 2000–2010, Journal of Geophysical Research: Biogeosciences, 117, https://doi.org/10.1029/2011JG001901, https://agupubs.onlinelibrary.wiley.com/doi/abs/10.1029/2011JG001901, 2012.

Luo, Y., El-Madany, T. S., Filippa, G., Ma, X., Ahrens, B., Carrara, A., Gonzalez-Cascon, R., Cremonese, E., Galvagno, M., Hammer, T. W., Pacheco-Labrador, J., Martín, M. P., Moreno, G., Perez-Priego, O., Reichstein, M., Richardson, A. D., Römermann, C., and Migliavacca, M.: Using Near-Infrared-Enabled Digital Repeat Photography to Track Structural and Physiological Phenology in Mediterranean Tree–Grass Ecosystems, Remote Sensing, 10, 1293, https://doi.org/10.3390/rs10081293, https://www.mdpi.com/2072-4292/10/8/1293, 2018.

Marcolla, B., Pitacco, A., and Cescatti, A.: Canopy Architecture and Turbulence Structure in a Coniferous Forest, Boundary-Layer Meteorology, 108, 39–59, https://doi.org/10.1023/A:1023027709805, https://doi.org/10.1023/A:1023027709805, 2003.

Marcolla, B., Cescatti, A., Manca, G., Zorer, R., Cavagna, M., Fiora, A., Gianelle, D., Rodeghiero, M., Sottocornola, M., and Zampedri, R.: Climatic controls and ecosystem responses drive the inter-annual variability of the net ecosystem exchange of an alpine meadow, Agricultural and Forest Meteorology, 151, 1233–1243, https://doi.org/10.1016/j.agrformet.2011.04.015, http://www.sciencedirect.com/science/article/pii/S0168192311001444, 2011.

Marras, S., Pyles, R. D., Sirca, C., Paw U, K. T., Snyder, R. L., Duce, P., and Spano, D.: Evaluation of the Advanced Canopy–Atmosphere–Soil Algorithm (ACASA) model performance over Mediterranean maquis ecosystem, Agricultural and Forest Meteorology, 151, 730–745, https://doi.org/10.1016/j.agrformet.2011.02.004, http://www.sciencedirect.com/science/article/pii/S0168192311000566, 2011.

McDowell, N. G., Marshall, J. D., Hooker, T. D., and Musselman, R.: Estimating CO2 flux from snowpacks at three sites in the Rocky Mountains, Tree Physiology, 20, 745–753, https://doi.org/10.1093/treephys/20.11.745, https://academic.oup.com/treephys/article/20/11/745/1690523, 2000.

Merbold, L., Eugster, W., Stieger, J., Zahniser, M., Nelson, D., and Buchmann, N.: Greenhouse gas budget (CO2, CH4 and N2O) of intensively managed grassland following restoration, Global Change Biology, 20, 1913–1928, https://doi.org/10.1111/gcb.12518, https://onlinelibrary.wiley.com/doi/abs/10.1111/gcb.12518, _eprint: https://onlinelibrary.wiley.com/doi/pdf/10.1111/gcb.12518, 2014.

Migliavacca, M., Sonnentag, O., Keenan, T. F., Cescatti, A., O'Keefe, J., and Richardson, A. D.: On the uncertainty of phenological responses to climate change, and implications for a terrestrial biosphere model, Biogeosciences, 9, 2063–2083, https://doi.org/https://doi.org/10.5194/bg-9-2063-2012, https://www.biogeosciences.net/9/2063/2012/, 2012.

Molen, M. K. v. d., Huissteden, J. v., Parmentier, F. J. W., Petrescu, A. M. R., Dolman, A. J., Maximov, T. C., Kononov, A. V., Karsanaev, S. V., and Suzdalov, D. A.: The growing season greenhouse gas balance of a continental tundra site in the Indigirka lowlands, NE Siberia, Biogeosciences, 4, 985–1003, https://doi.org/https://doi.org/10.5194/bg-4-985-2007, https://www.biogeosciences.net/4/985/2007/, 2007.

Monson, R. K., Turnipseed, A. A., Sparks, J. P., Harley, P. C., Scott-Denton, L. E., Sparks, K., and Huxman, T. E.: Carbon sequestration in a high-elevation, subalpine forest, Global Change Biology, 8, 459–478, https://doi.org/10.1046/j.1365-2486.2002.00480.x, https://onlinelibrary.wiley.com/doi/abs/10.1046/j.1365-2486.2002.00480.x, 2002.

Montagnani, L., Manca, G., Canepa, E., Georgieva, E., Acosta, M., Feigenwinter, C., Janous, D., Kerschbaumer, G., Lindroth, A., Minach, L., Minerbi, S., Mölder, M., Pavelka, M., Seufert, G., Zeri, M., and Ziegler, W.: A new mass conservation approach to the study of CO2 advection in an alpine forest, Journal of Geophysical Research: Atmospheres, 114, https://doi.org/10.1029/2008JD010650, https://agupubs.onlinelibrary.wiley.com/doi/full/10.1029/2008JD010650, 2009.

Moors, E.: Water use of forests in the Netherlands, Tech. rep., Vrije Universiteit, Amsterdam, http://edepot.wur.nl/213926, 2012.

Morellato, L. P. C., Alberti, L. F., and Hudson, I. L.: Applications of Circular Statistics in Plant Phenology: a Case Studies Approach, in: Phenological Research, pp. 339–359, Springer, Dordrecht, https://doi.org/10.1007/978-90-481-3335-2_16, https://link.springer.com/chapter/10.1007/978-90-481-3335-2_16, 2010.

Morente-López, J., Lara-Romero, C., Ornosa, C., and Iriondo, J. M.: Phenology drives species interactions and modularity in a plant - flower visitor network, Scientific Reports, 8, 9386, https://doi.org/10.1038/s41598-018-27725-2, https://www.nature.com/articles/s41598-018-27725-2, 2018.

Morin, X., Roy, J., Sonié, L., and Chuine, I.: Changes in leaf phenology of three European oak species in response to experimental climate change, New Phytologist, 186, 900–910, https://doi.org/10.1111/j.1469-8137.2010.03252.x, https://nph.onlinelibrary.wiley.com/doi/abs/10.1111/j.1469-8137.2010.03252.x, 2010.

Musavi, T., Migliavacca, M., Weg, M. J. v. d., Kattge, J., Wohlfahrt, G., Bodegom, P. M. v., Reichstein, M., Bahn, M., Carrara, A., Domingues, T. F., Gavazzi, M., Gianelle, D., Gimeno, C., Granier, A., Gruening, C., Havránková, K., Herbst, M., Hrynkiw, C., Kalhori, A., Kaminski, T., Klumpp, K., Kolari, P., Longdoz, B., Minerbi, S., Montagnani, L., Moors, E., Oechel, W. C., Reich, P. B., Rohatyn, S., Rossi, A., Rotenberg, E., Varlagin, A., Wilkinson, M., Wirth, C., and Mahecha, M. D.: Potential and limitations of inferring ecosystem photosynthetic capacity from leaf functional traits, Ecology and Evolution, 6, 7352–7366, https://doi.org/10.1002/ece3.2479, https://onlinelibrary.wiley.com/doi/abs/10.1002/ece3.2479, _eprint: https://onlinelibrary.wiley.com/doi/pdf/10.1002/ece3.2479 tex.ids: musavi_potential_2016, 2016.

Pastorello, G., Papale, D., Chu, H., Trotta, C., Agarwal, D., Canfora, E., Baldocchi, D., and Torn, M.: A New Data Set to Keep a Sharper Eye on Land-Air Exchanges, Eos, https://doi.org/10.1029/2017EO071597, https://eos.org/project-updates/a-new-data-set-to-keep-a-sharper-eye-on-land-air-exchanges, 2017.

Peichl, M., Gažovič, M., Vermeij, I., Goede, E. d., Sonnentag, O., Limpens, J., and Nilsson, M. B.: Peatland vegetation composition and phenology drive the seasonal trajectory of maximum gross primary production, Scientific Reports, 8, 8012, https://doi.org/10.1038/s41598-018-26147-4, https://www.nature.com/articles/s41598-018-26147-4, 2018.

Peñuelas, J., Rutishauser, T., and Filella, I.: Phenology Feedbacks on Climate Change, Science, 324, 887–888, https://doi.org/10.1126/science.1173004, http://science.sciencemag.org/content/324/5929/887, 2009.

Pilegaard, K., Ibrom, A., Courtney, M. S., Hummelshøj, P., and Jensen, N. O.: Increasing net CO2 uptake by a Danish beech forest during the period from 1996 to 2009, Agricultural and Forest Meteorology, 151, 934–946, https://doi.org/10.1016/j.agrformet.2011.02.013, http://www.sciencedirect.com/science/article/pii/S0168192311000797, 2011.

Post, E. and Forchhammer, M. C.: Climate change reduces reproductive success of an Arctic herbivore through trophic mismatch, Philosophical Transactions of the Royal Society B: Biological Sciences, 363, 2367–2373, https://doi.org/10.1098/rstb.2007.2207, http://www.royalsocietypublishing.org/doi/10.1098/rstb.2007.2207, 2008.

Prescher, A.-K., Grünwald, T., and Bernhofer, C.: Land use regulates carbon budgets in eastern Germany: From NEE to NBP, Agricultural and Forest Meteorology, 150, 1016–1025, https://doi.org/10.1016/j.agrformet.2010.03.008, http://www.sciencedirect.com/science/article/pii/S0168192310000961, 2010.

Rambal, S., Joffre, R., Ourcival, J. M., Cavender-Bares, J., and Rocheteau, A.: The growth respiration component in eddy CO2 flux from a Quercus ilex mediterranean forest, Global Change Biology, 10, 1460–1469, https://doi.org/10.1111/j.1365-2486.2004.00819.x, https://onlinelibrary.wiley.com/doi/abs/10.1111/j.1365-2486.2004.00819.x, 2004.

Reichstein, M., Falge, E., Baldocchi, D., Papale, D., Aubinet, M., Berbigier, P., Bernhofer, C., Buchmann, N., Gilmanov, T., Granier, A., Grünwald, T., Havránková, K., Ilvesniemi, H., Janous, D., Knohl, A., Laurila, T., Lohila, A., Loustau, D., Matteucci, G., Meyers, T., Miglietta, F., Ourcival, J.-M., Pumpanen, J., Rambal, S., Rotenberg, E., Sanz, M., Tenhunen, J., Seufert, G., Vaccari, F., Vesala, T., Yakir, D., and Valentini, R.: On the separation of net ecosystem exchange into assimilation and ecosystem respiration: review and improved algorithm, Global Change Biology, 11, 1424–1439, https://doi.org/10.1111/j.1365-2486.2005.001002.x, https://onlinelibrary.wiley.com/doi/abs/10.1111/j.1365-2486.2005.001002.x, 2005.

Rey, A., Pegoraro, E., Tedeschi, V., Parri, I. D., Jarvis, P. G., and Valentini, R.: Annual variation in soil respiration and its components in a coppice oak forest in Central Italy, Global Change Biology, 8, 851–866, https://doi.org/10.1046/j.1365-2486.2002.00521.x, https://onlinelibrary.wiley.com/doi/abs/10.1046/j.1365-2486.2002.00521.x, 2002.

Richardson, A. D., Braswell, B. H., Hollinger, D. Y., Jenkins, J. P., and Ollinger, S. V.: Near-surface remote sensing of spatial and temporal variation in canopy phenology, Ecological Applications, 19, 1417–1428, https://doi.org/10.1890/08-2022.1, https://esajournals.onlinelibrary.wiley.com/doi/abs/10.1890/08-2022.1, 2009.

Richardson, A. D., Andy Black, T., Ciais, P., Delbart, N., Friedl, M. A., Gobron, N., Hollinger, D. Y., Kutsch, W. L., Longdoz, B., Luyssaert, S., Migliavacca, M., Montagnani, L., William Munger, J., Moors, E., Piao, S., Rebmann, C., Reichstein, M., Saigusa, N., Tomelleri, E., Vargas, R., and Varlagin, A.: Influence of spring and autumn phenological transitions on forest ecosystem productivity, Philosophical Transactions of the Royal Society B: Biological Sciences, 365, 3227–3246, https://doi.org/10.1098/rstb.2010.0102, http://www.royalsocietypublishing.org/doi/10.1098/rstb.2010.0102, 2010.

Richardson, A. D., Keenan, T. F., Migliavacca, M., Ryu, Y., Sonnentag, O., and Toomey, M.: Climate change, phenology, and phenological control of vegetation feedbacks to the climate system, Agricultural and Forest Meteorology, 169, 156–173, https://doi.org/10.1016/j.agrformet.2012.09.012, http://www.sciencedirect.com/science/article/pii/S0168192312002869https://ac.els-cdn.com/S0168192312002869/1-s2.0-S0168192312002869-main.pdf?_tid=76d74384-1176-11e8-af6a-00000aacb35f&acdnat=1518606293_09713e0dfdf7faf8bd98f605a02a234fhttps://www.scienced, 2013.

Ryan, E. M., Ogle, K., Zelikova, T. J., LeCain, D. R., Williams, D. G., Morgan, J. A., and Pendall, E.: Antecedent moisture and temperature conditions modulate the response of ecosystem respiration to elevated CO2 and warming, Global Change Biology, 21, 2588–2602, https://doi.org/10.1111/gcb.12910, https://onlinelibrary.wiley.com/doi/abs/10.1111/gcb.12910, 2015.

Saleska, S. R., Miller, S. D., Matross, D. M., Goulden, M. L., Wofsy, S. C., da Rocha, H. R., de Camargo, P. B., Crill, P., Daube, B. C., de Freitas, H. C., Hutyra, L., Keller, M., Kirchhoff, V., Menton, M., Munger, J. W., Pyle, E. H., Rice, A. H., and Silva, H.: Carbon in Amazon Forests: Unexpected Seasonal Fluxes and Disturbance-Induced Losses, Science, 302, 1554–1557, https://doi.org/10.1126/science.1091165, https://science.sciencemag.org/content/302/5650/1554, tex.eprint: https://science.sciencemag.org/content/302/5650/1554.full.pdf tex.publisher: American Association for the Advancement of Science, 2003.

Schimel, D., Pavlick, R., Fisher, J. B., Asner, G. P., Saatchi, S., Townsend, P., Miller, C., Frankenberg, C., Hibbard, K., and Cox, P.: Observing terrestrial ecosystems and the carbon cycle from space, Global Change Biology, 21, 1762–1776, https://doi.org/10.1111/gcb.12822, https://onlinelibrary.wiley.com/doi/abs/10.1111/gcb.12822, 2015.

Schmid, H. P., Grimmond, C. S. B., Cropley, F., Offerle, B., and Su, H.-B.: Measurements of CO2 and energy fluxes over a mixed hardwood forest in the mid-western United States, Agricultural and Forest Meteorology, 103, 357–374, https://doi.org/10.1016/S0168-1923(00)00140-4, http://www.sciencedirect.com/science/article/pii/S0168192300001404, 2000.

Scott, R. L., Cable, W. L., and Hultine, K. R.: The ecohydrologic significance of hydraulic redistribution in a semiarid savanna, Water Resources Research, 44, https://doi.org/10.1029/2007WR006149, https://agupubs.onlinelibrary.wiley.com/doi/abs/10.1029/2007WR006149, 2008.

Serrano-Ortiz, P., Domingo, F., Cazorla, A., Were, A., Cuezva, S., Villagarcía, L., Alados-Arboledas, L., and Kowalski, A. S.: Interannual CO2 exchange of a sparse Mediterranean shrubland on a carbonaceous substrate, Journal of Geophysical Research: Biogeosciences, 114, https://doi.org/10.1029/2009JG000983, https://agupubs.onlinelibrary.wiley.com/doi/abs/10.1029/2009JG000983, 2009.

Suni, T., Rinne, J., Reissell, A., Altimir, N., Keronen, P., Rannik, U., Dal Maso, M., Kulmala, M., and Vesala, T.: Long-term measurements of surface fluxes above a Scots pine forest in Hyytiala, southern Finland, 1996-2001, BOREAL ENVIRONMENT RESEARCH, 8, {287–301}, tex.orcid-numbers: Vesala, Timo/0000-0002-4852-7464 Kulmala, Markku/0000-0003-3464-7825 Rinne, Janne/0000-0003-1168-7138 Dal Maso, Miikka/0000-0003-3040-3612 Keronen, Petri/0000-0001-5019-0904 tex.researcherid-numbers: Vesala, Timo/C-3795-2017 Kulmala, Markku/I-7671-2016 Rinne, Janne/A-6302-2008 Dal Maso, Miikka/A-7980-2008 tex.unique-id: ISI:000221372700003, 2003.

Tedeschi, V., Rey, A., Manca, G., Valentini, R., Jarvis, P. G., and Borghetti, M.: Soil respiration in a Mediterranean oak forest at different developmental stages after coppicing, Global Change Biology, 12, 110–121, https://doi.org/10.1111/j.1365-2486.2005.01081.x, https://onlinelibrary.wiley.com/doi/abs/10.1111/j.1365-2486.2005.01081.x, 2006.

Thum, T., Aalto, T., Laurila, T., Aurela, M., Kolari, P., and Hari, P.: Parametrization of two photosynthesis models at the canopy scale in a northern boreal Scots pine forest, Tellus B, 59, 874–890, https://doi.org/10.1111/j.1600-0889.2007.00305.x, https://onlinelibrary.wiley.com/doi/abs/10.1111/j.1600-0889.2007.00305.x, 2007.

Treuhaft, R. N., Law, B. E., and Asner, G. P.: Forest Attributes from Radar Interferometric Structure and Its Fusion with Optical Remote Sensing, BioScience, 54, 561–571, https://doi.org/10.1641/0006-3568(2004)054[0561:FAFRIS]2.0.CO;2, https://academic.oup.com/bioscience/article/54/6/561/294539, 2004.

Urbanski, S., Barford, C., Wofsy, S., Kucharik, C., Pyle, E., Budney, J., McKain, K., Fitzjarrald, D., Czikowsky, M., and Munger, J. W.: Factors controlling CO2 exchange on timescales from hourly to decadal at Harvard Forest, Journal of Geophysical Research: Biogeosciences, 112, https://doi.org/10.1029/2006JG000293, https://agupubs.onlinelibrary.wiley.com/doi/full/10.1029/2006JG000293, 2007.

Valentini, R., Angelis, P. D., Matteucci, G., Monaco, R., Dore, S., and Mucnozza, G. E. S.: Seasonal net carbon dioxide exchange of a beech forest with the atmosphere, Global Change Biology, 2, 199–207, https://doi.org/10.1111/j.1365-2486.1996.tb00072.x, https://onlinelibrary.wiley.com/doi/abs/10.1111/j.1365-2486.1996.tb00072.x, 1996.

Von Mises, R.: Über die 'Ganzzahligkeit' der Atomgewichte und verwandte Fragen, Physikalische Zeitschrift, 19, 490–500, 1918.

Wang, X. and Wu, C.: Estimating the peak of growing season (POS) of China's terrestrial ecosystems, Agricultural and Forest Meteorology, 278, 107 639, https://doi.org/10.1016/j.agrformet.2019.107639, http://www.sciencedirect.com/science/article/pii/S0168192319302473, 2019.

Wohlfahrt, G., Hammerle, A., Haslwanter, A., Bahn, M., Tappeiner, U., and Cernusca, A.: Seasonal and inter-annual variability of the net ecosystem CO2 exchange of a temperate mountain grassland: Effects of weather and management, Journal of Geophysical Research: Atmospheres, 113, https://doi.org/10.1029/2007JD009286, https://agupubs.onlinelibrary.wiley.com/doi/abs/10.1029/2007JD009286, 2008.

Xu, L. and Baldocchi, D. D.: Seasonal trends in photosynthetic parameters and stomatal conductance of blue oak (Quercus douglasii) under prolonged summer drought and high temperature, Tree Physiology, 23, 865–877, https://doi.org/10.1093/treephys/23.13.865, https://academic.oup.com/treephys/article/23/13/865/1650675, 2003.

Xu, L. and Baldocchi, D. D.: Seasonal variation in carbon dioxide exchange over a Mediterranean annual grassland in California, Agricultural and Forest Meteorology, 123, 79–96, https://doi.org/10.1016/j.agrformet.2003.10.004, http://www.sciencedirect.com/science/article/pii/S0168192303002533, 2004.

Zhang, X., Friedl, M. A., Schaaf, C. B., Strahler, A. H., Hodges, J. C. F., Gao, F., Reed, B. C., and Huete, A.: Monitoring vegetation phenology using MODIS, Remote Sensing of Environment, 84, 471–475, https://doi.org/10.1016/S0034-4257(02)00135-9, http://www.sciencedirect.com/science/article/pii/S0034425702001359, 2003.

Zhou, S., Zhang, Y., Caylor, K. K., Luo, Y., Xiao, X., Ciais, P., Huang, Y., and Wang, G.: Explaining inter-annual variability of gross primary productivity from plant phenology and physiology, Agricultural and Forest Meteorology, 226-227, 246–256, https://doi.org/10.1016/j.agrformet.2016.06.010, http://www.sciencedirect.com/science/article/pii/S0168192316303070, 2016.

Zhou, S., Zhang, Y., Ciais, P., Xiao, X., Luo, Y., Caylor, K. K., Huang, Y., and Wang, G.: Dominant role of plant physiology in trend and variability of gross primary productivity in North America, Scientific Reports, 7, 41 366, https://doi.org/10.1038/srep41366, https://www.nature.com/articles/srep41366, 2017.

Zielis, S., Etzold, S., Zweifel, R., Eugster, W., Haeni, M., and Buchmann, N.: NEP of a Swiss subalpine forest is significantly driven not only by current but also by previous year's weather, Biogeosciences, 11, 1627–1635, https://doi.org/https://doi.org/10.5194/bg-11-1627-2014, https://www.biogeosciences.net/11/1627/2014/, publisher: Copernicus GmbH, 2014.

Code availability. Code will be made available under GPL-3 license upon publication

Data availability. FLUXNET database is available in the web page: https://fluxnet.fluxdata.org/

Author contributions. DEPM, TM, MM, and MDM designed the study in collaboration with MR and CR. DEPM conducted the analysis and wrote the manuscript with substantial contributions from all co-authors

Competing interests. The authors declare that they have no conflict of interest